



Inhibiting CDK4/6 in pancreatic ductal adenocarcinoma via microRNA-21

Maria Mortoglou^a, Francesc Miralles^b, Rhys Richard Mould^c, Dipankar Sengupta^d, Pinar Uysal-Onganer^{a,*}

^a Cancer Mechanisms and Biomarkers Research Group, School of Life Sciences, University of Westminster, W1W 6UW London, UK

^b Centre of Biomedical Education/Molecular and Clinical Sciences, Cell Biology Research Centre, St. George's, University of London, Cranmer Terrace, London SW17 0RE, UK

^c Research Centre for Optimal Health, School of Life Sciences, University of Westminster, W1W 6UW London, UK

^d Health Data Sciences Research Group, Research Centre for Optimal Health, School of Life Sciences, University of Westminster, W1W 6UW London, UK

ARTICLE INFO

Keywords:

PDAC
Palbociclib
MicroRNAs
CDK4/6 inhibition
Apoptosis
Cell cycle
Senescence
Proliferation

ABSTRACT

Pancreatic ductal adenocarcinoma (PDAC) is one of the most aggressive malignancies, with a 5-year survival rate of 5–10%. The high mortality rate is due to the asymptomatic progression of clinical features in metastatic stages of the disease, which renders standard therapeutic options futile. PDAC is characterised by alterations in several genes that drive carcinogenesis and limit therapeutic response. The two most common genetic aberrations in PDAC are the mutational activation of KRAS and loss of the tumour suppressor CDK inhibitor 2A (*CDKN2A*), which culminate the activation of the cyclin-dependent kinase 4 and 6 (CDK4/6), that promote G1 cell cycle progression. Therapeutic strategies focusing on the CDK4/6 inhibitors such as palbociclib (PD-0332991) may potentially improve outcomes in this malignancy. MicroRNAs (miRs/miRNAs) are small endogenous non-coding RNA molecules associated with cellular proliferation, invasion, apoptosis, and cell cycle. Primarily, miR-21 promotes cell proliferation and a higher proportion of PDAC cells in the S phase, while knockdown of miR-21 has been linked to cell cycle arrest at the G2/M phase and inhibition of cell proliferation. In this study, using a CRISPR/Cas9 loss-of-function screen, we individually silenced the expression of miR-21 in two PDAC cell lines and in combination with PD-0332991 treatment, we examined the synergetic mechanisms of CDK4/6 inhibitors and miR-21 knockouts (KOs) on cell survival and death. This combination reduced cell proliferation, cell viability, increased apoptosis and G1 arrest in vitro. We further analysed the mitochondrial respiration and glycolysis of PDAC cells; then assessed the protein content of these cells and revealed numerous Kyoto Encyclopedia of Genes and Genomes (KEGG) pathways associated with PD-0332991 treatment and miR-21 knocking out. Our results demonstrate that combined targeting of CDK4/6 and silencing of miR-21 represents a novel therapeutic strategy in PDAC.

1. Introduction

Pancreatic ductal adenocarcinoma (PDAC) is the most common type of pancreatic cancer (PCa), which accounts for about 85% of pancreatic tumours (Sevgin et al., 2021). PDAC is predicted to be the second

leading cause of cancer mortality by 2030 (Rahib et al., 2014), while only 10–20% of PDAC are resectable at diagnosis. Response to chemotherapy is generally poor (Stark et al., 2016; Strobel et al., 2022) due to multifactorial reasons such as diagnosis at late stages, rapid progression of metastasis, and resistance to conventional therapeutic

Abbreviations: BRCA2, Breast cancer gene 2; CDK, Cyclin-Dependent Kinases; CDK4/6, Cyclin-dependent kinase 4 and 6; CDKN2A, CDK inhibitor 2 A; CycD, D-cyclins; DMEM, Dulbecco's Modified Eagle's Medium; DMSO, Dimethyl sulfoxide; EGF, Epidermal growth factor; ERK, Extracellular signal-regulated kinase; ESCC, Esophageal squamous cell carcinoma; FBS, Foetal bovine serum; 5-FU, 5-fluorouracil; GO, Gene Ontology; HR+, Hormone receptor-positive; KEGG, Kyoto Encyclopedia of Genes and Genomes; KOs, Knockouts; MAPK, microRNAs, Mitogen-activated protein kinasemiRs/miRNAs; mTOR, Mammalian/mechanistic target of rapamycin; MTT, 3-(4,5-dimethylthiazol-2-yl)-2,5-diphenyltetrazolium bromide; NF- κ B, Nuclear factor- κ B; OCR, Oxygen consumption rate; PARP, Poly (ADP-ribose) polymerase; PBS, Phosphate buffered saline; PCa, Pancreatic cancer; PD-0332991, Palbociclib; PDAC, Pancreatic ductal adenocarcinoma; PDX, Patient-derived xenografts; PI, Propidium iodide; PI3K, Phosphatidylinositol 3-kinase; PKM2, Isoform M2 of pyruvate kinase; RB, Retinoblastoma; SA-miRs, Senescence-associated miRs; SD, Standard deviation; TP53, Tumour protein 53; VEGF, Vascular endothelial growth factor.

* Corresponding author.

E-mail address: p.onganer@westminster.ac.uk (P. Uysal-Onganer).

<https://doi.org/10.1016/j.ejcb.2023.151318>

Received 20 February 2023; Received in revised form 17 April 2023; Accepted 22 April 2023

Available online 25 April 2023

0171-9335/© 2023 The Author(s). Published by Elsevier GmbH. This is an open access article under the CC BY-NC-ND license (<http://creativecommons.org/licenses/by-nc-nd/4.0/>).

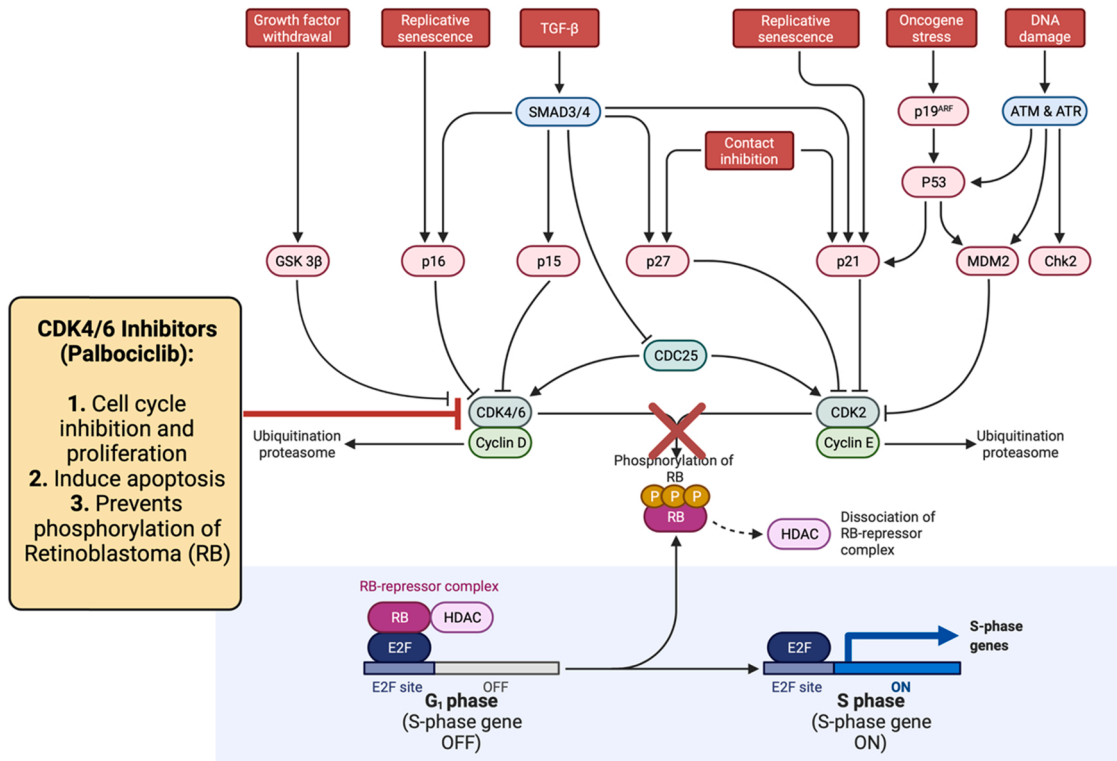


Fig. 1. CDK4/6 inhibitors for PDAC therapy. D-cyclins (CycD) activate CDK4 and CKD6 in the G1 phase and stimulate cell cycle progression through the phosphorylation of the RB. In PDAC, CDK4/6 is overactivated, which leads to uncontrolled cell proliferation. CDK4/6 inhibitors have been shown to promote an effective therapeutic activity via the repression of CDK4/6 expression and the inhibition of cell proliferation. Using CDK4/6 inhibitors combined with targeting other signalling pathways may promote a pioneer strategy against therapy resistance. Created with BioRender.com.

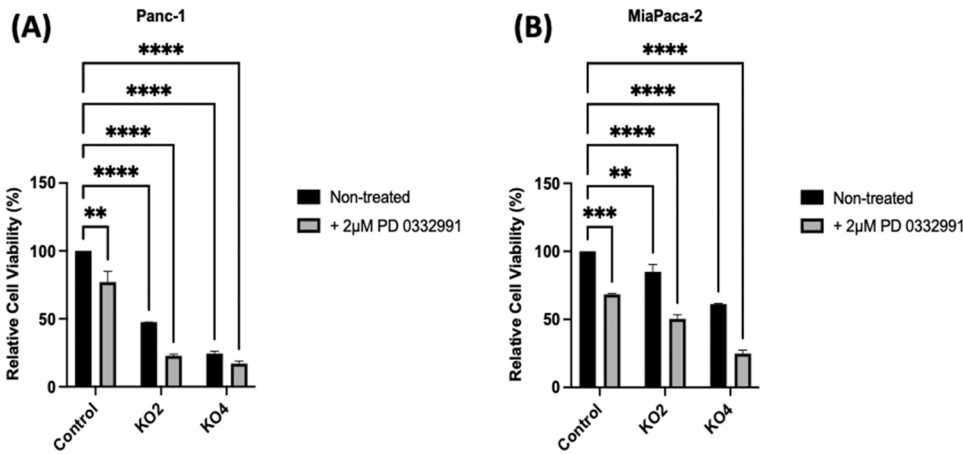


Fig. 2. PD-0332991 decreased cell viability in Panc-1 and MiaPaCa-2 wt cells and their miR-21 KO2. Panc-1 (A) and MiaPaCa-2 (B) were treated with PD-0332991 (2 µM, for 24 hrs). Cells were incubated for 24 hrs and analysed by the MTT method. Cellular viability of treated Panc-1 miR-21 KO2 was also decreased by 50 % compared to non-treated Panc-1 miR-21 KO2 (n = 3; p ≤ 0.01), however mir-21 KO4 did not show the similar trend. Cellular viability of treated MiaPaCa-2 miR-21 KO2 and KO4 was also decreased by 40 % and 59 % compared to non-treated MiaPaCa-2 miR-21 KO2 and KO4 (n = 3; p ≤ 0.0001, for all), respectively. The data are the mean ± SD of three technical repeats evaluated by One-way ANOVA and Bonferroni's multiple comparison test. Exact p-values are indicated * p ≤ 0.05; ** p ≤ 0.01; *** p ≤ 0.001; **** p ≤ 0.0001; error bars indicate SD.

modalities (Ma and Jemal, 2013). Systemic therapy for PDAC includes chemotherapy drugs such as gemcitabine, taxanes and molecular-targeted agents such as erlotinib (O'Hayer and Brody, 2016; Von Hoff et al., 2013). Current therapies also comprise DNA-damaging agents comprising gemcitabine (6.8 months median survival), folinic acid (11.1 months median survival), 5-fluorouracil [5-FU], irinotecan, or oxaliplatin and microtubule poisons such as albumin-bound paclitaxel (Nab-paclitaxel), which have limited increase in overall survival (Conroy et al., 2018; Garrido-Laguna and Hidalgo, 2015).

Large-scale genomic studies have identified recurrent genetic alterations in PDAC, such as activation of oncogenes (mutant KRAS is found in >90 % of PDAC) and inactivation of tumour suppressor genes tumour

protein 53 (TP53), p16/CDK inhibitor 2A (CDKN2A), SMAD4, and breast cancer gene 2 (BRCA2) in >50 % of PDAC cases) (Bailey et al., 2016a; Biankin et al., 2012; Cicens et al., 2017; Jaffee et al., 2002; Maitra and Hruban, 2008; Waddell et al., 2015; Witkiewicz et al., 2015a). Specifically, aberrations in the oncogenic KRAS (proto-oncogene, GTPase) gene result in the activation of the cyclin-dependent kinases (CDK) and the mammalian/mechanistic target of the rapamycin (mTOR) signalling pathway, which are further linked to elevated cell survival (Bryant et al., 2014; Conway et al., 2019). The CDKN2A gene encodes p14/Arf and p16/Ink4a, which are potent inhibitors of CDK4 and CDK6 (Foulkes et al., 1997; Young et al., 2014). Mutated CDKN2A is the most common alteration in PDAC mouse models driven by oncogenic

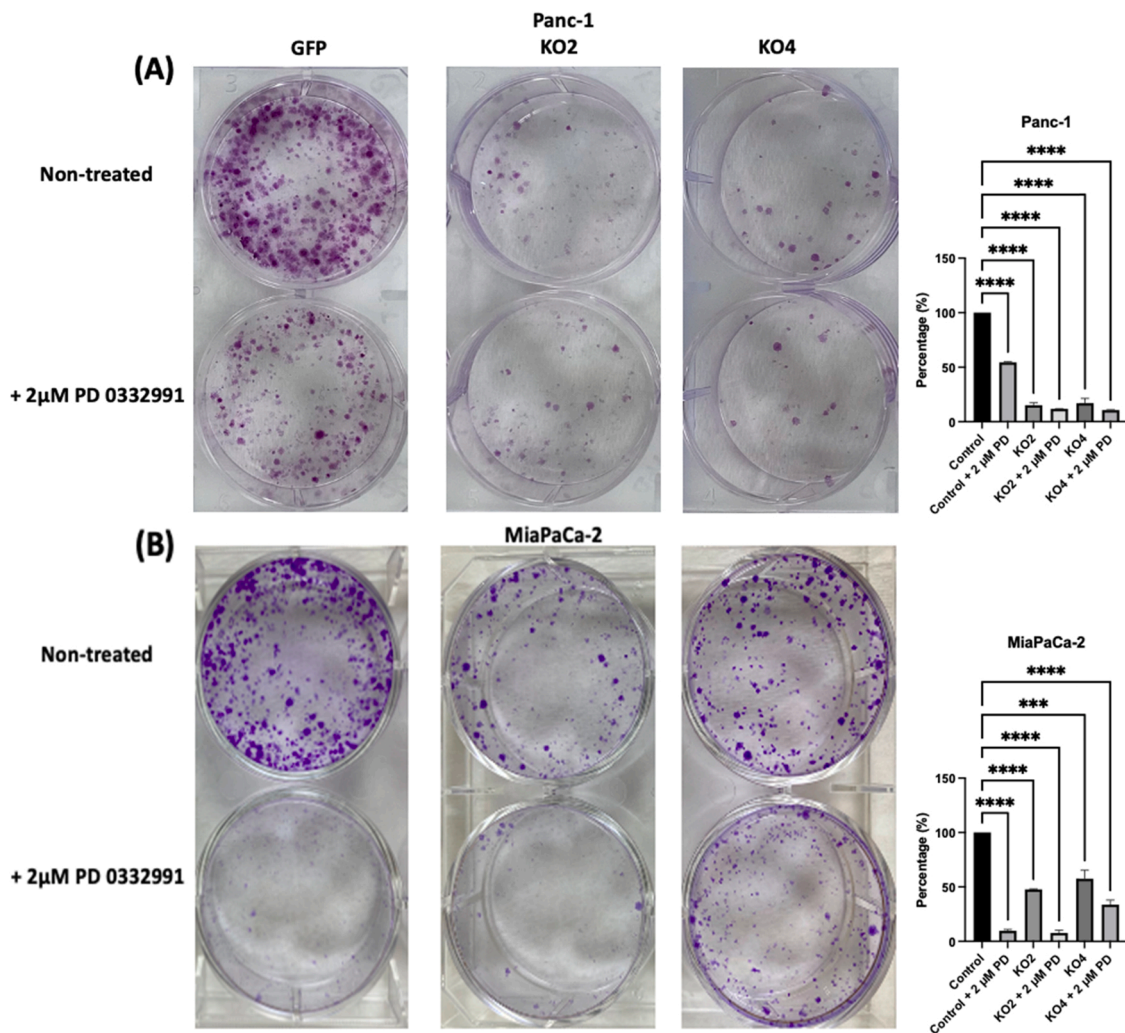


Fig. 3. PD-0332991 decreased colony formation in Panc-1 and MiaPaCa-2 wt cells and their miR-21 KOs. The colony formation of Panc-1 (A) and MiaPaCa-2 (B) cells was counted after 10 days of treatment with media replenishment every 2 days. Graphs show the colony numbers quantification as percentages normalised to the control. The histograms represented the mean \pm SD of three technical repeats; data evaluated by One-way ANOVA and Bonferroni's multiple comparison test. Panc-1 and MiaPaCa-2 cells were exposed to PD-0332991 (2 μ M, for 24 h). Exact p-values are indicated * $p \leq 0.05$; ** $p \leq 0.01$; *** $p \leq 0.001$; **** $p \leq 0.0001$; error bars indicate SD.

KRAS (Mueller et al., 2018), suggesting the relevance of activating CDK4/6 to promote cell-cycle entry. The loss of *CDK2NA* (p16) and tumour suppressor *TP53* in the cell cycle leads to uncontrolled cell proliferation, whereas mutations in *KRAS* and *TP53* play an important role in glucose metabolism, which disturbs cell maintenance (Bryant et al., 2014; Regel et al., 2012; Rivlin et al., 2011; Weissmueller et al., 2014). Hence, altered metabolic machinery in PDAC cells is a promising strategy for developing an effective therapy and disease management. Genetic alteration in PDAC results in the dysregulation of CDK4 and CDK6 through the inactivation of retinoblastoma (RB), which is a tumour suppressor protein (Cowan and Maitra, 2014; Schutte et al., 1997; Witkiewicz et al., 2015a).

CDK4/6 inhibitors such as Palbociclib (PD-0332991), Ribociclib (LEE011), and Abemaciclib (LY2835219) are being examined as novel therapeutic agents in more than 300 preclinical and clinical trials for more than 50 different types of malignancies (Fassl et al., 2022). It has been shown that PD-0332991 displays antiproliferative activity in PDAC cell lines and patient-derived xenografts (PDX) (Chou et al., 2018; Heilmann et al., 2014; Knudsen et al., 2019; Witkiewicz et al., 2015b). PD-0332991 has been also approved as a therapeutic agent for advanced metastatic hormone receptor-positive (HR+)/HER2-negative breast cancer (Eggersmann et al., 2019; Franco et al., 2014; Goel et al., 2018).

Specifically, CDK4/6 inhibitors can induce apoptosis and are linked to canonical effects, including cell cycle inhibition and proliferation (Bonelli, 2019; Dhir et al., 2019; Franco et al., 2014; Musgrove et al., 2011). Recent studies have revealed that PD-0332991 is also associated with non-canonical functions such as reversible senescence, metabolic rearrangement, and immunomodulation (Bonelli et al., 2019; Skowron et al., 2020), which could be pioneer approaches for cancer therapy (Nardella et al., 2011; Shao et al., 2019). During carcinogenesis, activating upstream mitogenic pathways, which elevate CDK4/6 activity leads to therapy resistance (Feng and Kurokawa, 2019; Niu et al., 2019). Especially, mitogenic signals from receptor tyrosine kinases and downstream signalling events including RAS, phosphatidylinositol 3-kinase (PI3K), mitogen-activated protein kinase (MAPK) and mTOR progress the quiescent cells from G0 or G1 phase into S phase through CDK4 or CDK6 complex (Lim and Kaldis, 2013; Malumbres and Barbacid, 2001; Rodgers et al., 2014). Therefore, the continuous activation of cell cycle-related signalling pathways allows the utility of CDK inhibitors as therapeutic agents in cancer treatment (Jingwen et al., 2017) (Fig. 1).

MicroRNAs (miRs/miRNAs) are small non-coding RNAs, which can regulate gene expression at the post-transcriptional level (Krol et al., 2010). Several studies have shown that miRs play an important role in numerous biological processes during carcinogenesis, such as

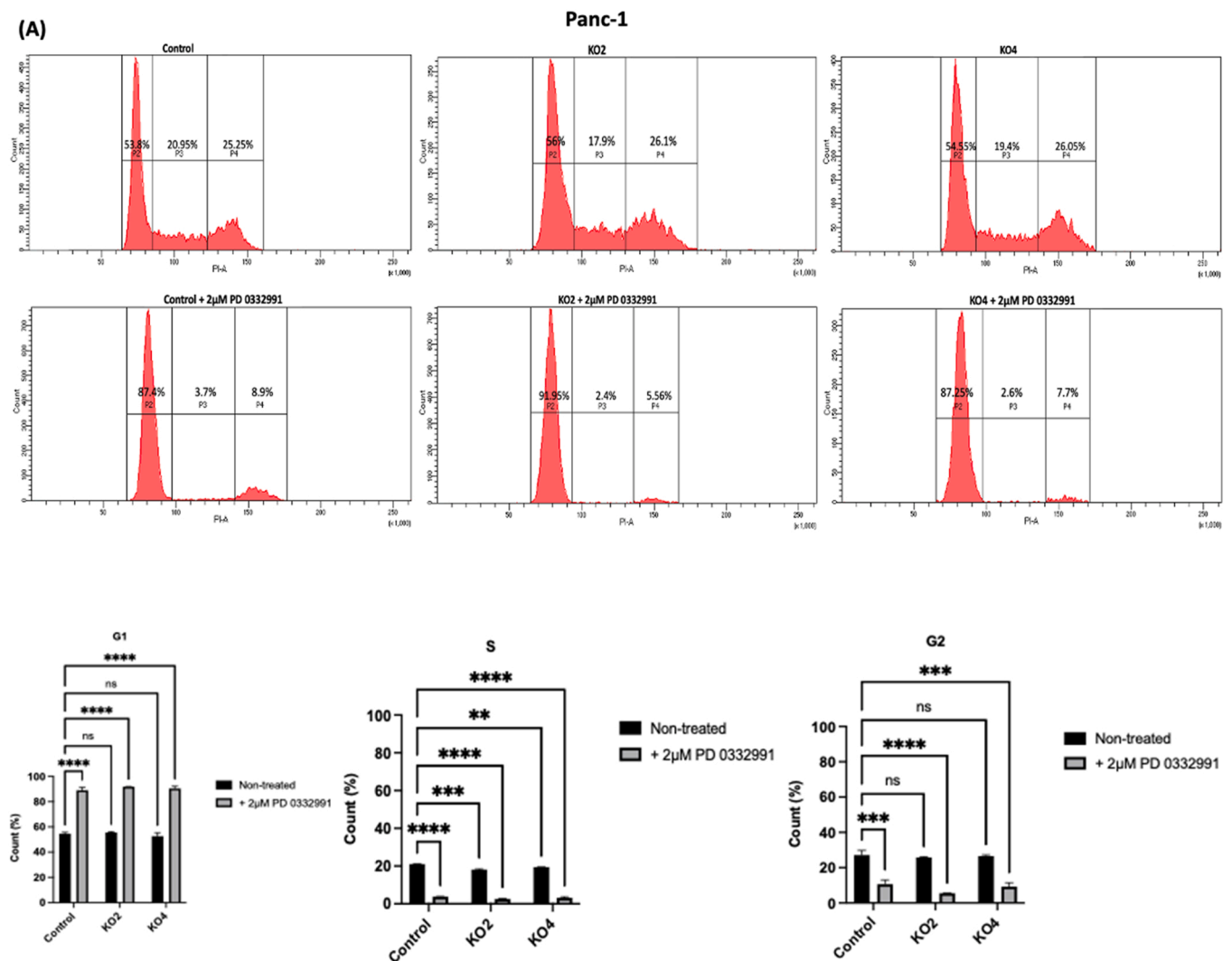


Fig. 4. PD-0332991 induced cell cycle arrest in Panc-1 (A) and MiaPaCa-2 (B) wt cells and miR-21 KOs. Cells were treated with PD-0332991 (2 μ M, for 24 h). After drug treatment, cells were fixed with 70 % EtOH at +4 $^{\circ}$ C for a week and stained with PI. The histograms represented the mean \pm SD of three technical repeats; data evaluated by One-way ANOVA and Bonferroni's multiple comparison test. Exact p-values are indicated * $p < 0.05$; ** $p < 0.01$; *** $p < 0.001$; **** $p < 0.0001$; error bars indicate SD.

proliferation, differentiation, invasion, migration, and apoptosis through the modulation of specific target mRNA expressions (Iorio and Croce, 2009). Evidence demonstrates that miR-21 is an oncogenic miR presenting the highest specificity (0.80) and sensitivity (0.77) as an early PDAC diagnostic marker out of 7 key candidates (hsa-miR-31-5p, hsa-miR-210-3p and hsa-miR-155-5p, hsa-miR-217, hsa-miR-148a-3p and hsa-miR-375) (Qu et al., 2017; Zhou et al., 2014). Additionally, miR-21 promotes carcinogenesis by regulating cell cycle, apoptosis, invasion, and metastasis (Asangani et al., 2008; Liu et al., 2009). miR-21 confers resistance against CDK4/6 inhibitors and prevents their therapeutic efficiency. Previous reports indicated that thymic tumours of mTOR knock-down mice were characterised by upregulation of miR-21 and let-7a miRs and undetectable levels of the CDK6 protein. These tumour cells with reduced mTOR activity demonstrated greater resistance to treatment with PD-0332991 than tumour cells from mTOR wild-type mice. mTOR inhibition resulted in let-7 and miR-21 upregulation and consequent repression of CDK6 (Gary et al., 2020). Collectively, genetic, or pharmacological downregulation of mTOR resulted in let-7 and miR-21 increase and subsequently in downregulation of CDK6. Accordingly, simultaneous inhibition of the mTOR pathway and CDK6 activity by PD-0332991 exerted greater antitumor activity than either

treatment alone, both in vitro in human T-cell acute lymphoblastic leukaemia/lymphoma and in vivo (Gary et al., 2020).

Since PDAC is a molecularly-diverse disease showing several genetic alterations, understanding the mechanisms underlying PDAC carcinogenesis is crucial for early diagnosis, risk stratification, and targeted therapeutic strategies (Bailey et al., 2016b; Cancer Genome Atlas, 2017; Jones et al., 2008; Knudsen et al., 2016). In this study, we aimed to evaluate the therapeutic potential of PD-0332991 in two PDAC cell lines (Panc-1 and MiaPaCa-2 cells) with different genetic features; and assess the synergistic effects of PD-0332991 treatment and miR-21 knockout not only in cellular proliferation, survival, cell cycle arrest, senescence, apoptosis, glycolytic and oxidative metabolism but also the protein content between the different samples (treated/non-treated wt control cells, treated/non-treated miR-21 KO2 cells).

2. Materials and methods

2.1. Cell culture and reagents

Panc-1 (ATCC[®] CRL-1469[™]) and MiaPaCa-2 (ATCC[®] CRL-x1420[™]) cell lines were cultured according to ATCC's recommendations to 80 %

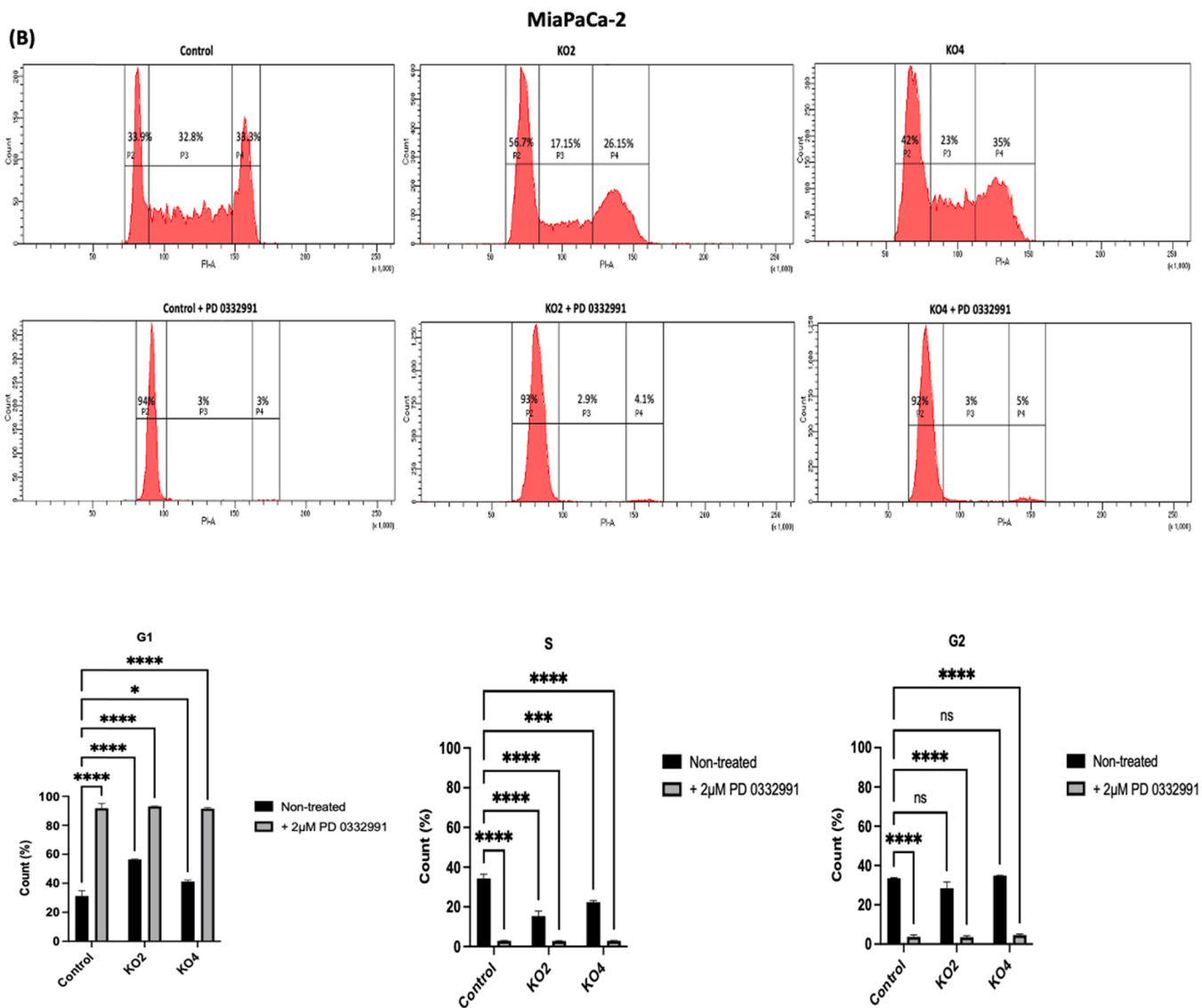


Fig. 4. (continued).

Table 1

Percentage of Panc-1 cell population in cell cycle.

Cell Cycle Phase	Control	Control + PD-0332991	KO2	KO2 + PD-0332991	KO4	KO4 + PD-0332991
G1	53.8 %	87.4 %	56 %	91.95 %	54.55 %	87.25 %
S	20.95 %	3.7 %	17.9 %	2.4 %	19.4 %	2.6 %
G2	25.25 %	8.9 %	26.1 %	5.56 %	26.05 %	7.7 %

Table 2

Percentage of MiaPaCa-2 cell population in cell cycle.

Cell Cycle Phase	Control	Control + PD-0332991	KO2	KO2 + PD-0332991	KO4	KO4 + PD-0332991
G1	33.9 %	94 %	56.7 %	93 %	42 %	92 %
S	32.8 %	3 %	17.15 %	2.9 %	23 %	3 %
G2	33.3 %	3 %	26.15 %	4.1 %	35 %	5 %

confluence in 75 cm² flasks in complete Dulbecco's Modified Eagle's Medium (DMEM), with 10 % foetal bovine serum (FBS) at 37 °C with 5 % CO₂. PD-0332991 was purchased from Selleck Chemicals (Houston, TX, USA) and was dissolved in dimethyl sulfoxide (DMSO) at an initial

stock concentration of 10 mM and stored as aliquots at -20 °C.

2.2. CRISPR/Cas9 assay

The CRISPR/Cas9-mediated miR-21 gene editing vectors encoding four different gRNAs, eGFP (control), and Cas9 protein, were kindly provided by Dr Junming Yue, University of Tennessee Health Science Centre, USA, and produced based on the recommendations of previously published studies (Arisan et al., 2021; Huo et al., 2017; Yue et al., 2010). Stable cell lines were generated as described before and selected with puromycin (1–10 µg/mL). The specific clones have been chosen as previously described (Arisan et al., 2021).

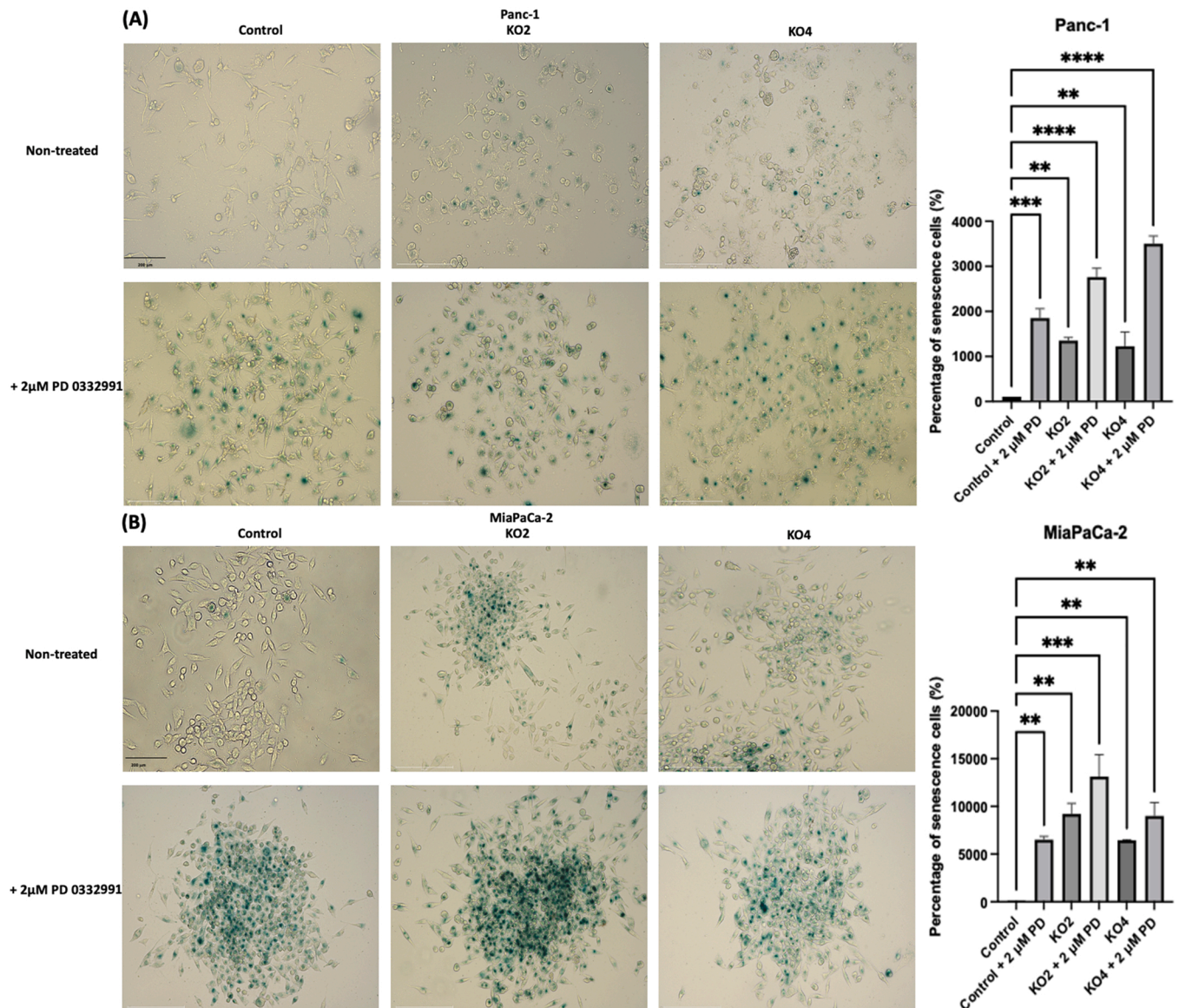


Fig. 5. PD-0332991 treatment triggered cellular senescence in both Panc-1 (A) and MiaPaCa-2 (B) wt cells and their miR-21 KOs. Panc-1 and MiaPaCa-2 wt cells and their miR-21 KOs were exposed to Senescence β -Galactosidase Staining following treatment with the CDK4/6 inhibitor PD-0332991 (2 μ M, for 24 hrs). After a night of Senescence β -Galactosidase staining, cells were examined under a light microscope. The scale bar is 200 μ m. Graphs show the cell numbers quantification normalised to the control. The histograms represented the mean \pm SD of three technical repeats; data evaluated by One-way ANOVA and Bonferroni's multiple comparison test. Panc-1 and MiaPaCa-2 cells were exposed to PD-0332991 (2 μ M, for 24 hrs). Exact p-values are indicated * $p \leq 0.05$; ** $p \leq 0.01$; *** $p \leq 0.001$; **** $p \leq 0.0001$; error bars indicate SD.

2.3. Cell viability assay

The effects of the CDK4/6 inhibitor PD-0332991 on Panc-1 and MiaPaCa-2 cell lines wt and their knockouts (KOs) were determined by a colorimetric MTT (3-(4,5-dimethylthiazol-2-yl)-2,5-diphenyltetrazolium bromide) assay. The cells were seeded at a density of 1×10^4 cells per well in 96-well plates and treated with PD-0332991 (2 μ M, for 24 hrs) as previously described (Mortoglou et al., 2022; Rencuzogullari et al., 2020). Then, 10 μ l of MTT dye [5 mg/mL in phosphate-buffered saline (PBS), Sigma; St. Louis, MO, USA] was added to the culture medium and incubated at 37 $^{\circ}$ C for 4 h. To solubilize the formazan crystals converted from MTT by the mitochondrial enzymes, 100 μ l DMSO (Sigma; St. Louis, MO, USA) was added. The absorbance of the suspension at 570 nm was measured with a microplate reader (Bio-Rad, Hercules, CA, USA).

2.4. Colony formation assay

Panc-1 and MiaPaCa-2 wt and their miR-21 KOs were seeded at 3×10^3 cells/well in 6-well plates and allowed to adhere for 24 hrs. After attachment, the cells were treated with PD-0332991 (2 μ M, for 24 hrs). After 24 hrs, drug-containing media were removed, and the cells were allowed to form colonies in complete media for 10 days. The colony numbers were quantified by using Image J.

2.5. Caspase activity assay

Measurements of caspase activities in Panc-1 and MiaPaCa-2 wt and their miR-21 KOs were performed using the commercially available Caspase-Glo 3/7 Assay (Promega, Madison, WI), according to the manufacturer's instructions. Cells were harvested after 24hrs incubation with PD-0332991 (2 μ M) and subjected to caspase-3 activity detection.

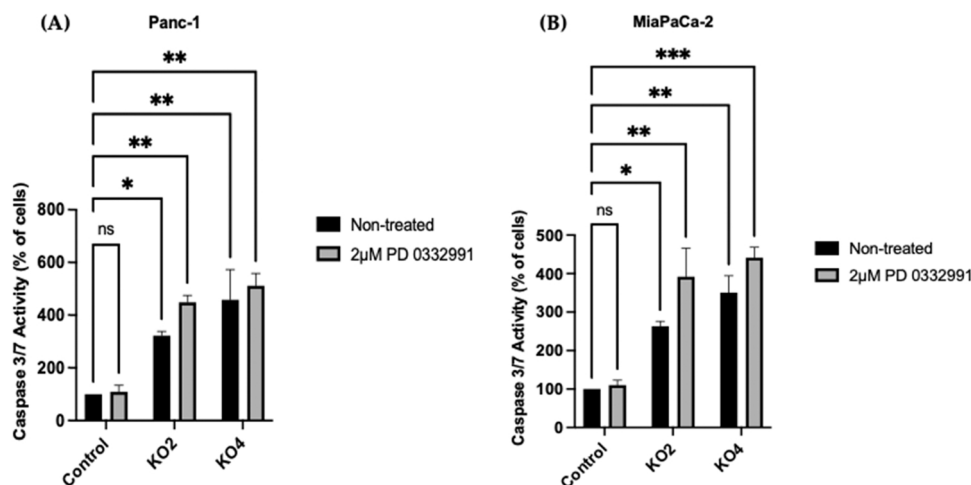


Fig. 6. Effects of PD-0332991 on apoptotic cell death. Panc-1 (A) and MiaPaCa-2 (B) wt cells and their miR-21 KO2 were treated with PD-0332991 (2 μ M, for 24 hrs), and the caspase 3–7 activities were analysed. The histograms represented the mean \pm SD from three technical repeats; data evaluated by One-way ANOVA and Bonferroni's multiple comparison test. Exact p-values are indicated * $p \leq 0.05$; ** $p \leq 0.01$; *** $p \leq 0.001$; **** $p \leq 0.0001$; error bars indicate SD.

Specifically, Caspase-Glo® 3/7 Assay reagent (100 μ l) was prepared according to the Caspase-Glo® 3/7 Assay Technical Bulletin TB323 and added to each well. Plates were briefly shaken and incubated at room temperature for 1 hr. Caspase-Glo® 3/7 luminescent signal was read on the BMG FLUOstar OPTIMA (BMG Labtech, Ortenberg, Germany). Background signal (media-only wells) was subtracted from all values and mean \pm standard deviation (SD) were calculated from triplicates.

2.6. Cell cycle analysis by flow cytometry

Panc-1 and MiaPaCa-2 wt and their miR-21 KO2 were seeded at 5×10^4 in 6-well plates and exposed to PD-0332991 (2 μ M, for 24 hrs). Following trypsinization, the cells were centrifuged at 2000 rpm for 5 min. The cells were then fixed with 70 % ethanol and incubated at 4 $^{\circ}$ C until the analysis (Rencuzogullari et al., 2020). Later, the cells were stained with propidium iodide (PI)/RNase staining buffer for 30 min and analysed by a flow cytometer (BD Accuri Bioscience, Franklin Lakes, NJ, USA). Results were analysed using BD LSRFortessa X-20 (BD Bioscience, U.K.).

2.7. Senescence β -galactosidase staining

Panc-1 and MiaPaCa-2 wt and their miR-21 KO2 were seeded as 3×10^5 cells in 6-well plates and were treated with PD-0332991 (2 μ M, for 24 hrs). After 24 hrs of drug exposure, the medium was removed, and the cells were washed twice with 1X PBS. Cells were fixed according to the protocol indicated by Senescence β -Galactosidase (SA- β) Staining Kit #9860 (CST, Danvers, MA, USA). Then, cells were microscopically examined after β -gal administration using EVOS FL Auto 2 Imaging System (ThermoFisher, U.K.) (Dhir et al., 2019; Yuedi et al., 2020). The cell numbers were calculated by using ImageJ.

2.8. Wound healing assay

Panc-1 and MiaPaCa-2 wt and their miR-21 KO2 were seeded at 80 % density cells/well in 24-well plates until cells reached monolayer confluence and then were exposed to PD-0332991 (2 μ M, for 24 hrs). A straight scratch on the cell monolayers was created using a sterile 10 μ l pipette tip to obtain a wound in the monolayer. Detached cells were washed with 1 \times PBS gently, and cells were then supplemented with a renewed medium containing 5 % v/v FBS and incubated at 37 $^{\circ}$ C. Wound closure was observed every 24 hrs until the wound closed using EVOS FL Auto 2 Imaging System (ThermoFisher, U.K.) ($\times 10$). The program was used for analysing the wound area at different time points and

presented by bar graphics using GraphPad software (v.9).

2.9. XF Cell mito stress test

Oxygen consumption rate (OCR) was measured using the Seahorse XF Cell Mito Stress Test Kit (Agilent, UK) according to the manufacturer's instructions. Briefly, Panc-1 and MiaPaCa-2 wt and miR-21 KO2 cells were seeded in XF24 cell culture microplates at 4×10^4 cells/well density until cells reached monolayer confluence. After the treatment of the cells with PD-0332991 (2 μ M, for 24 h), the culture medium was replaced with Seahorse XF Base Medium (Agilent, U.K.), 2 mM glutamine, 1 mM sodium pyruvate and 10 mM glucose, pH 7.4) and the plate was pre-incubated for 1 h at 37 $^{\circ}$ C in a non-CO₂ incubator. OCR was measured under basal conditions, and then after sequential injections of different reagents, where their concentrations were optimised for each cell line as: 1.5 μ M oligomycin (respiratory Complex V inhibitor that allows for the calculation of adenosine triphosphate (ATP) production by mitochondria), 2.5 μ M (Panc-1 cells) and 3 μ M (MiaPaCa-2 cells) carbonyl cyanide-p-trifluoromethoxy-phenyl-hydrazon (FCCP; an uncoupling agent allowing determination of the maximal respiration and the spare capacity), and finally a combination of 1 μ M rotenone and 1 μ M antimycin A (Complex I and III inhibitors, respectively) to stop mitochondrial respiration enabling the calculation of the background (i. e., non-mitochondrial respiration driven by processes outside the mitochondria). Wave Software (version 2.6.3) was used to design, run, and view results from the MitoStress assay. OCR measurements were normalised to protein content using the Bradford Assay carried out as follows: after the measurements, cells were collected, lysed in RIPA (Sigma-Aldrich, Gillingham, U.K., containing 10 % protease inhibitor cocktail, Sigma-Aldrich) and quantified by Bradford Assay.

2.10. Protein isolation and LC-MS/MS proteomic analysis

Total protein was extracted from treated and Panc-1 and MiaPaCa-2 wt cells and their miR-21 KO2 by using RIPA + buffer (Sigma, U.K.), which was supplemented with 10 % protease inhibitor complex (Sigma, U.K.). Samples were pipetting gently at regular intervals, while continuously shaking the cell preparation on ice for 2 hrs. Then, the cell preparations were centrifuged at $16,000 \times g$ at 4 $^{\circ}$ C for 30 min to collect the supernatants containing the extracted proteins. In-gel digestion was used for LC-MS/MS analysis, carried out by the Cambridge Centre for Proteomics (University of Cambridge, Cambridge, U.K.). The samples were prepared 1:1 in reducing Laemmli sample buffer (BioRad; containing 5 % β -mercaptoethanol, Sigma-Aldrich, U.K.), boiled and run

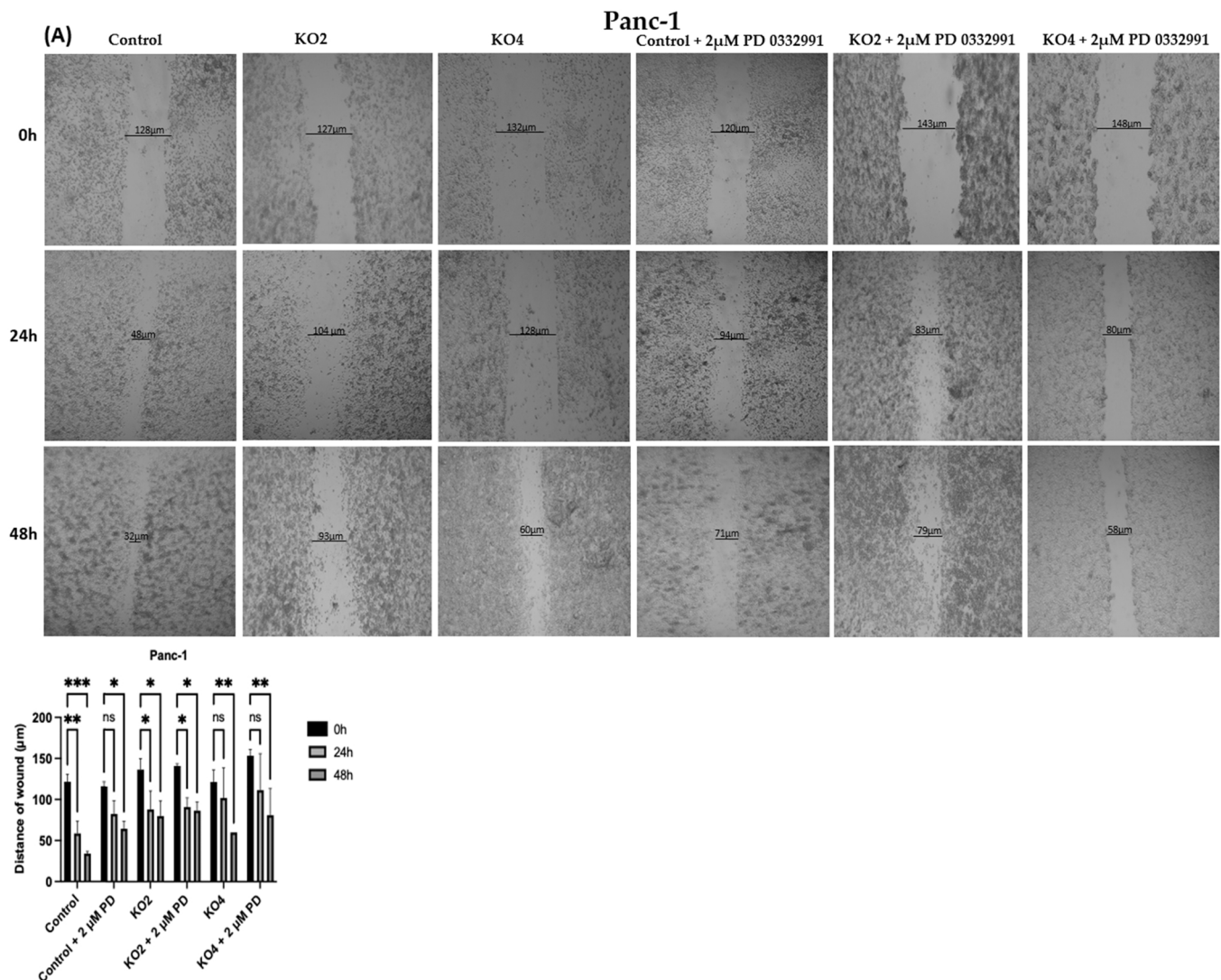


Fig. 7. PD-0332991 decreased the motility of Panc-1 (A) and MiaPaCa-2 (B) wt cells and their miR-21 KO2s. Wound healing assay was performed to compare the motility of Panc-1 and MiaPaCa-2 cells and their miR-21 KO2s with/out PD-0332991. Images were obtained by using EVOS FL Auto 2 Imaging System (ThermoFisher, U.K.) with x10 magnification. The scale bar is 200 μm . The average distance of wound area was shown following measurement of at least 5 different areas for 0, 24, and 48 hrs incubation time. Each data point represents the mean \pm SD of three technical repeats; data evaluated by One-way ANOVA and Bonferroni's multiple comparison test. Exact p-values are indicated * $p \leq 0.05$; ** $p \leq 0.01$; *** $p \leq 0.001$; **** $p \leq 0.0001$; error bars indicate SD.

0.5 cm into a 10 % TGX gel (BioRad, U.K.), and then cut out as one whole band per sample in both Panc-1 and MiaPaCa-2 PDAC cell lines (treated/non-treated wt control cells, treated/non-treated miR-21 KO2 cells). Proteomic analysis was carried out by the Cambridge Centre for Proteomics (Cambridge, U.K.) according to previously described methods (Pamenter et al., 2019). Protein scores are derived from ion scores as a non-probabilistic basis for ranking protein hits; individual ion scores >30 indicated identity or extensive homology ($p < 0.05$). An R-script was written to analyse the proteins expressed under four different conditions (treated/non-treated wt control cells, treated/non-treated miR-21 KO2 cells) for the two PDAC cell lines (Panc-1 and MiaPaCa-2). For each cell line, we identified the proteins that are uniquely expressed for each of these conditions and the ones that are expressed under all the conditions. This R-script is open access (GPU v.3 licence) and can be downloaded from <https://github.com/d-sengupt/ProteomicProfileComparison.git>.

2.11. Protein interaction network analysis

To identify local network clusters (STRING), gene ontology (GO) and Kyoto Encyclopedia of Genes and Genomes (KEGG) pathways for proteins from treated with PD-0332991 and non-treated Panc-1 and MiaPaCa-2 wt and their miR-21 KO2s, STRING analysis was used (<https://string-db.org/>, accessed on October 2022). Predicted protein interaction networks were built based on hits identified from the LC-MS/MS analysis using the protein IDs and organism choice *Homo sapiens* in the STRING software. For protein lists, "multiple proteins" was selected, confidence set at "medium," and network interaction connecting lines were based on known and predicted interactions. Protein networks were annotated for pathway analysis and data were exported as labelled network images for KEGG and/or Excel files for KEGG and Reactome pathways and STRING network clusters.

2.12. Statistical analysis

All the statistical analysis of the experiments were performed using

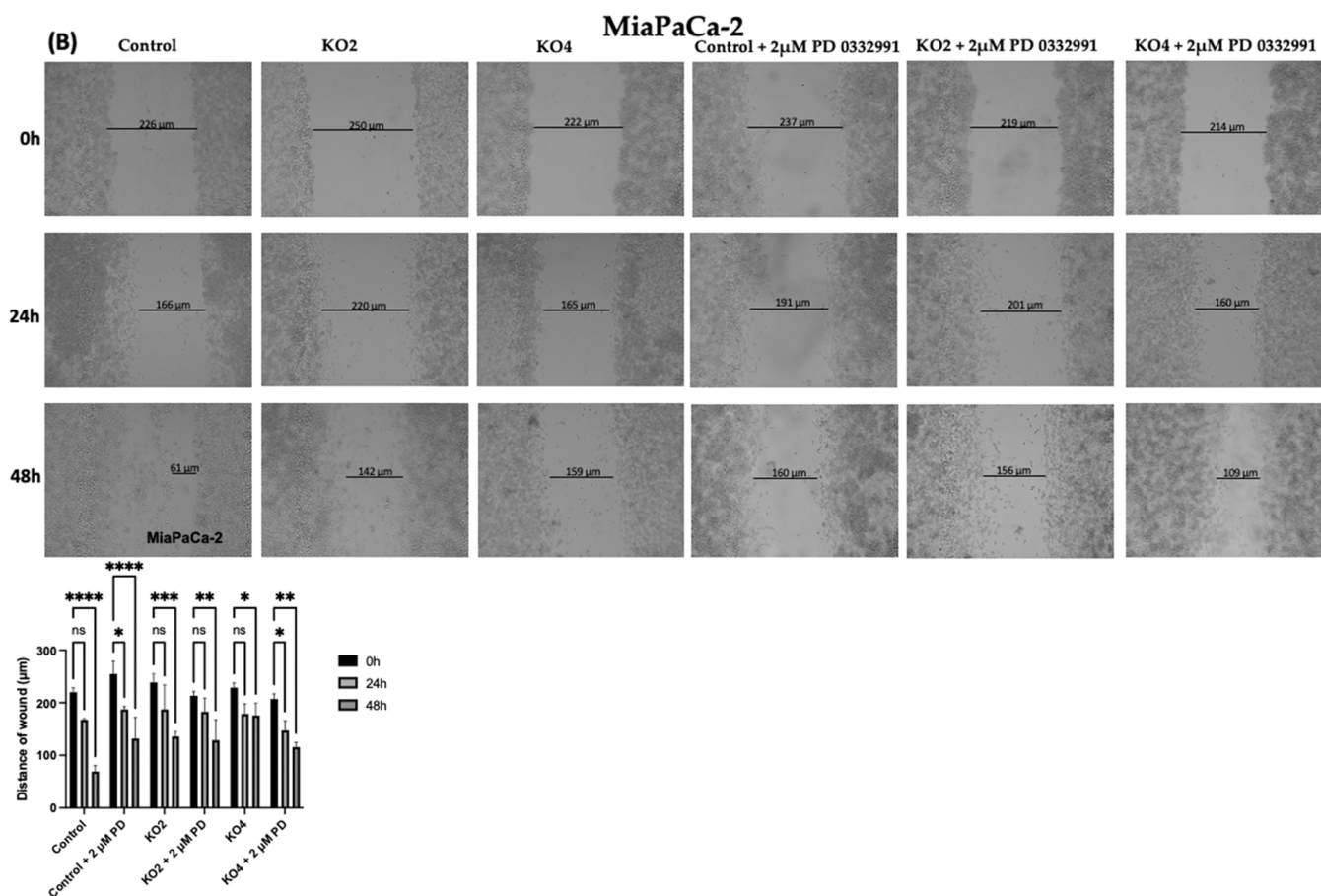


Fig. 7. (continued).

free commercially available software packages GraphPad Prism v9 (La Jolla, CA, USA). One-way ANOVA and Bonferroni multiple comparisons tests followed by Tukey's post-hoc analysis were used, whereas statistical significance was conducted as Tukey at $p \leq 0.05$. All the results were presented as mean \pm SD.

3. Results

3.1. PD-0332991 reduced cell viability and proliferation in PDAC cell lines and their miR-21 KOs

In our previous studies, we have found that miR-21 was highly upregulated in both Panc-1 and MiaPaCa-2 cell lines compared to normal pancreatic cell line (HPDE) (Mortoglou et al., 2022). Therefore, in this study, we examined the effect of PD-0332991 treatment on relative cell viability and colony-forming ability in Panc-1 and MiaPaCa-2 PDAC wt cells and their miR-21 KOs, we used MTT and colony formation assays. Panc-1 and MiaPaCa-2 wt cells and their miR-21 KOs were treated with PD-0332991 (2 μ M, for 24 hrs) as has been previously optimised (Sevgin et al., 2021; Rencuzogullari et al., 2020). We found that PD-0332991 treatment significantly decreased cellular viability of Panc-1 wt cells by 22.9 % ($n = 3$; $p \leq 0.01$), miR-21 KO2 by 77.2 % and miR-1 KO4 cells by 83 % ($n = 3$; $p \leq 0.0001$, for all) (Fig. 2 A). In MiaPaCa-2 cells, PD-0332991 treatment significantly reduced cellular viability of MiaPaCa-2 wt cells by 31.7 % ($n = 3$; $p \leq 0.001$), miR-21 KO2 by 49.6 % and miR-21 KO4 by 75.16 % ($n = 3$; $p \leq 0.0001$, for all). miR-21 deletion alone significantly reduced the cellular viability of PDAC cells. Panc-1 miR-21 KO2 and KO4 decreased cellular viability by 52.45 % and 75.6 %, respectively ($n = 3$; $p \leq 0.0001$, for all). MiaPaCa-2 miR-21 KO2 and KO4 showed a similar

trend by reducing cell viability by 15 % and 38.76 %, respectively ($n = 3$; $p \leq 0.01$, for KO2; $p \leq 0.001$, for KO4). Moreover, a combination of PD-0332991 treatment and miR-21 deletion resulted in a higher suppression of cellular viability in both Panc-1 and MiaPaCa-2 cells (Fig. 2B).

Then, we conducted a colony-forming assay to examine the long-term effects of both PD-0332991 treatment (2 μ M, for 24 hrs) and miR-21 KO. In line with the MTT assay results, PD-0332991 treatment significantly reduced the number of colonies in the Panc-1 wt cells, miR-21 KO2 and miR-21 KO4 by 46 %, 89 % and 90 %, respectively ($n = 3$; $p \leq 0.0001$ for all) compared to non treated Panc-1 wt cells. Panc-1 miR-21 KO2 and KO4 alone also significantly reduced the number of colony formations by 84.5 % and 83 %, respectively ($n = 3$; $p \leq 0.0001$ for all) (Fig. 3 A). In the MiaPaCa-2 cell line, PD-0332991 treatment remarkably reduced the potential of colony formation of the treated MiaPaCa-2 wt cells, miR-21 KO2 and miR-21 KO4 cells by 90 %, 92 % and 66 %, respectively ($n = 3$; $p \leq 0.0001$ for all). MiaPaCa-2 miR-21 KO2 and miR-21 KO4 alone also significantly reduced the colony numbers by 52 % ($n = 3$; $p \leq 0.0001$) and 42.5 %, respectively ($n = 3$; $p \leq 0.001$ for all) (Fig. 3B). The combination of PD-0332991 treatment and miR-21 KOs presented a more efficient therapeutic effect in the reduction of the colony formation in Panc-1 and MiaPaCa-2 cells.

3.2. PD-0332991 in combination with miR-21 KOs arrest the cell cycle and led to senescence

Flow cytometry was used to examine the effect of PD-0332991 on the cell cycle progression in Panc-1 and MiaPaCa-2 wt cells and their miR-21 KOs. To assess the effect of the CDK4/6 inhibitor on cell cycle distribution, we treated Panc-1, MiaPaCa-2 wt cells and their miR-21 KOs

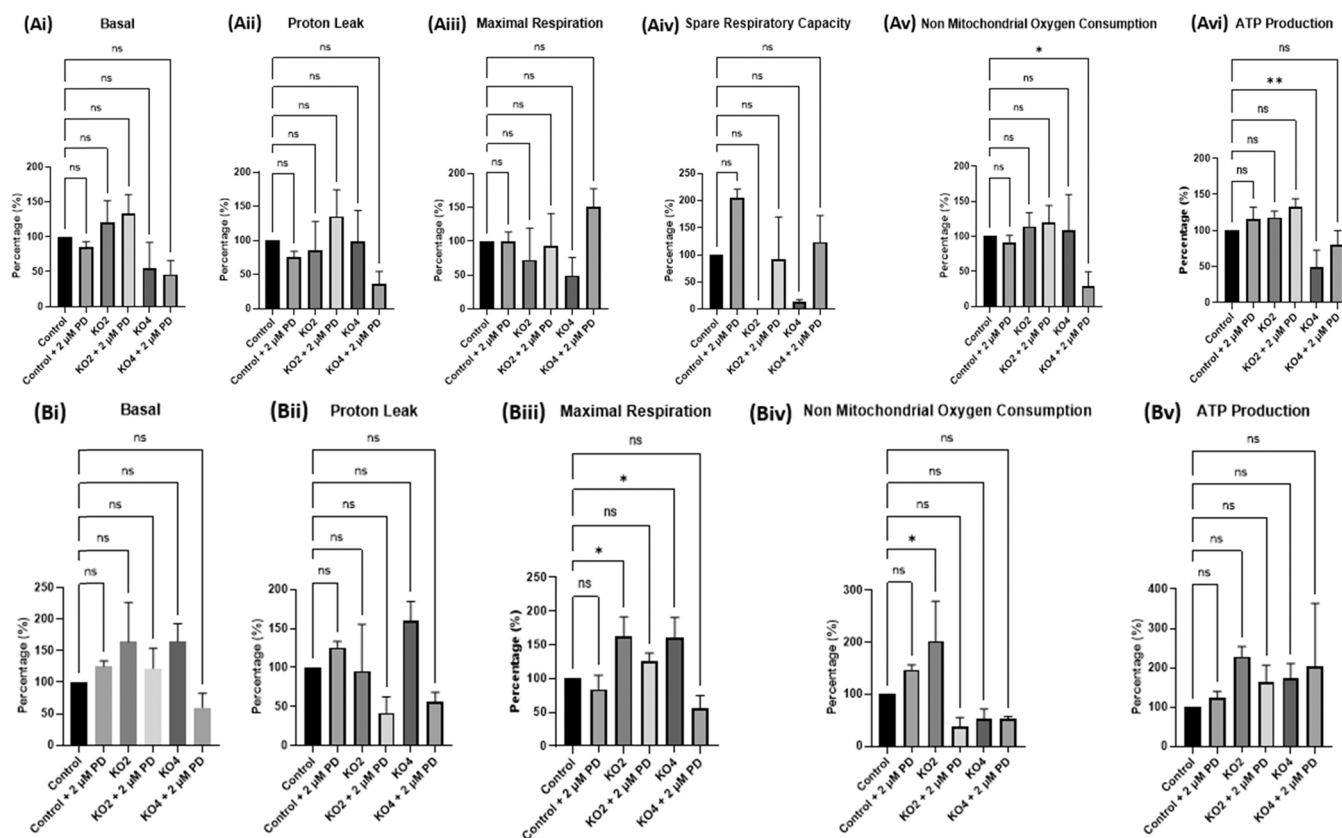


Fig. 8. Mitochondrial respiration function parameters of (A) Panc-1 cells and (B) MiaPaCa-2 cells and their miR-21 KO cells (KO2, KO4) treated with PD-0332991 (2 μM, for 24 hrs) using the Seahorse XFe24 extracellular flux analyzer. Changes of mitochondrial respiration were analysed with (i) basal respiration, (ii) proton leak, (iii) maximal respiration, (iv) spare respiratory capacity, (v) non mitochondrial oxygen consumption and (vi) ATP production. The data are the mean ± SD of three technical repeats and three biological repeats evaluated by One-way ANOVA and Bonferroni's multiple comparison test. Exact p-values are indicated * p ≤ 0.05; ** p ≤ 0.01; *** p ≤ 0.001; **** p ≤ 0.0001; error bars indicate SD.

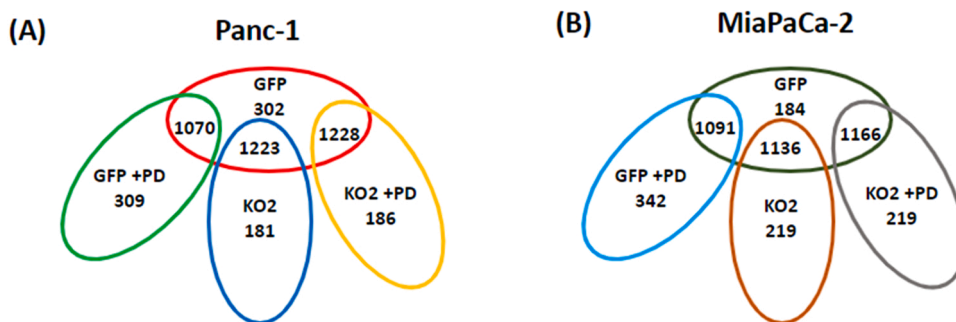


Fig. 9. Venn diagram comparing the accession numbers of proteins (unique and shared protein hits) identified in four different conditions (GFP, GFP + PD-0332991, miR-21 KO2, miR-21 KO2 + PD-0332991) in both Panc-1 (A) and MiaPaCa-2 (B) PDAC cell lines.

with PD-0332991 (2 μM, for 24 h). In the Panc-1 cell line, PD-0332991 treatment increased G1 cell cycle arrest by 34.45 %, 37.3 % and 35.9 % in Panc-1 wt cells, miR-21 KO2 and miR-21 KO4, respectively ($n = 3$; $p \leq 0.0001$, for all), compared to non-treated Panc-1 wt cells. However, miR-21 deletion alone did not cause a significant G1 arrest in the Panc-1 cells. Additionally, both miR-21 deletion and PD-0332991 treatment suppressed the S phase. PD-0332991 treatment decreased the population of Panc-1 wt cells by 17.25 % ($n = 3$; $p \leq 0.0001$), miR-21 KO2 by 18.45 % ($n = 3$; $p \leq 0.0001$), and miR-21 KO4 by 17.83 % ($n = 3$; $p \leq 0.0001$) in S phase. miR-21 KO alone also reduced the population of Panc-1 miR-21 KO2 cells by 2.9 % ($n = 3$; $p \leq 0.001$) and by 1.6 % ($n = 3$; $p \leq 0.01$) in miR-21 KO4 cells in S phase, compared to Panc-1 wt cells. PD-0332991 treatment suppressed G2 phase by 16.55 % ($n = 3$;

$p \leq 0.001$) in Panc-1 wt cells, by 21.62 % ($n = 3$; $p \leq 0.0001$) in Panc-1 miR-21 KO2 and by 17.9 % ($n = 3$; $p \leq 0.001$) in Panc-1 miR-21 KO4 cells related to non-treated Panc-1 wt cells. Nonetheless, miR-21 knocking out alone did not show a significant reduction in the population of Panc-1 cells in the G2 phase of the cell cycle (Fig. 4A, Table 1).

In the MiaPaCa-2 cell line, we showed that PD-0332991 treatment raised the G1 phase arrest rate by 60.5 % in MiaPaCa-2 wt cells, by 61.9 % in MiaPaCa-2 miR-21 KO2 and by 60.3 % in MiaPaCa-2 miR-21 KO4 ($n = 3$; $p \leq 0.0001$ for all), compared to the non-treated MiaPaCa-2 wt cells. Additionally, miR-21 deletion alone presented a significant contribution in G1 phase arrest by increasing G1 cell cycle arrest by 25.25 % ($n = 3$; $p \leq 0.0001$) in MiaPaCa-2 miR-21 KO2 cells and by 10.05 % ($n = 3$; $p \leq 0.05$) in MiaPaCa-2 miR-21 KO4 cells compared to

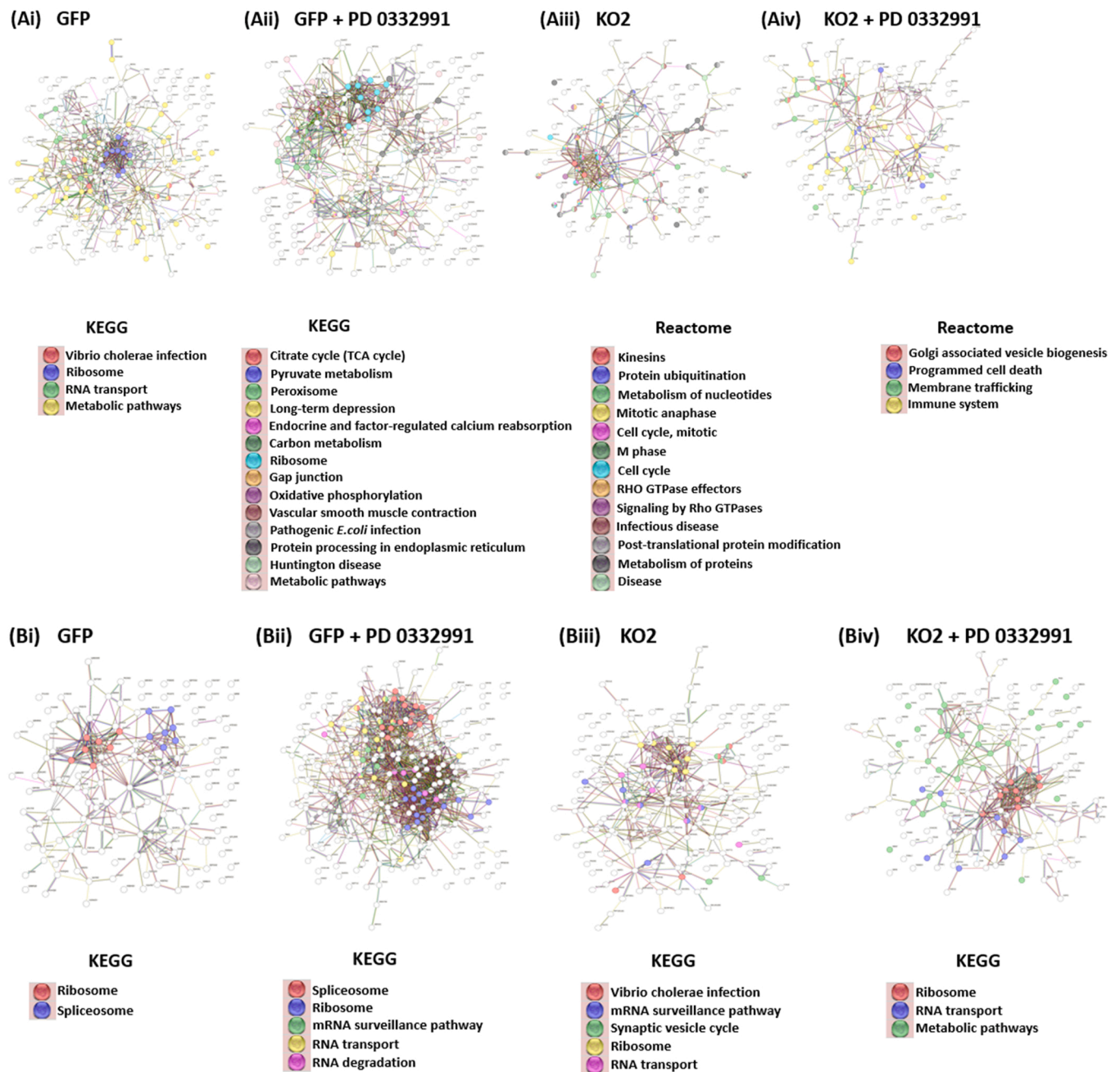


Fig. 10. KEGG and Reactome pathway analysis for protein network analysis for each examined group, presenting predicted protein networks annotating associated KEGG pathways for total protein of Panc-1 **(A)** **(Ai)** GFP **(Aii)** GFP + PD-0332991 **(Aiii)** miR-21 KO2 **(Aiv)** miR-21 KO2 + PD-0332991 and MiaPaCa-2 **(B)** **(Bi)** GFP **(Bii)** GFP + PD-0332991 **(Biii)** miR-21 KO2 **(Biv)** miR-21 KO2 + PD-0332991.

MiaPaCa-2 wt cells. We have also observed that miR-21 deletion alone and in combination with PD-0332991 treatment suppressed S cell cycle phase in MiaPaCa-2 cells. Specifically, PD-0332991 treatment suppressed S phase by 31.45 %, 31.5 % and 31.45 % in MiaPaCa-2 wt cells, miR-21 KO2 and miR-21 KO4, respectively compared to non-treated MiaPaCa-2 wt cells ($n = 3$; $p \leq 0.0001$, for all). Similarly, in MiaPaCa-2 cells, miR-21 deletion alone, repressed S phase by 18.93 % ($n = 3$; $p \leq 0.0001$) and 11.9 % ($n = 3$; $p \leq 0.001$) in MiaPaCa-2 miR-21 KO2 and miR-21 KO4, respectively. A same trend was detected in the G2 phase of MiaPaCa-2 cells, where PD-0332991 treatment suppressed G2 phase by 29.85 % ($n = 3$; $p \leq 0.0001$) in MiaPaCa-2 treated wt cells, by 30 % ($n = 3$; $p \leq 0.0001$) in MiaPaCa-2 miR-21 KO2 cells and by 28.95 % ($n = 3$; $p \leq 0.0001$) in MiaPaCa-2 miR-21 KO4 cells, compared to non-treated wt cells. Nevertheless, miR-21 deletion alone did not show

significant suppression of G2 phase in MiaPaCa-2 cells (Fig. 4B, Table 2).

We further examined the relationship between PD-0332991 treatment and the cellular senescence by performing a SA- β galactosidase test. After PD-0332991 treatment (2 μ M, for 24 h) in Panc-1 and MiaPaCa-2 wt cells and their miR-21 KO2 compared to non-treated wt cells. Panc-1 and MiaPaCa-2 treated wt cells and their treated miR-21 KO2 stained positively with SA- β Gal compared to non-treated wt cells. Moreover, both Panc-1 and MiaPaCa-2 miR-21 KO2 alone were stained positively with SA- β Gal (Fig. 5 A, B). Therefore, our results indicated that miR-21 KO2 alone and in combination with PD-0332991 treatment triggered further senescence in both PDAC cell lines.

Table 3

KEGG and Reactome pathways for total proteomic content of treated and non-treated with PD-0332991 Panc-1 and MiaPaCa-2 wt and miR-21 KO2s, as examined by LC-MS/MS analysis.

Panc-1 GFP	Panc-1 GFP+PD	Panc-1 KO2	Panc-1 KO2 +PD	MiaPaCa-2 GFP	MiaPaCa-2 GFP+PD	MiaPaCa-2 KO2	MiaPaCa-2 KO2 +PD
Metabolic pathways (45)	Citrate cycle (TCA cycle) (6)	Cell Cycle (20)	Membrane Trafficking (19)	Ribosome (7)	Spliceosome (18)	Ribosome (8)	Ribosome (10)
Ribosome (10)	Carbon metabolism (10)	Cell Cycle, Mitotic (17)	Golgi Associated Vesicle Biogenesis (7)	Spliceosome (7)	RNA transport (17)	mRNA surveillance pathway (7)	RNA transport (8)
RNA transport (10)	Ribosome (10)	Metabolism of proteins (34)	Immune System (31)		Ribosome (14)	RNA transport (8)	Metabolic pathways (30)
Vibrio cholerae infection (5)	Peroxisome (8)	Post-translational protein modification (26)	Programmed Cell Death (8)		mRNA surveillance pathway (10)	Vibrio cholerae infection (5)	
	Huntington disease (14)	M Phase (12)			RNA degradation (7)	Synaptic vesicle cycle (5)	
	Long-term depression (6)	Protein ubiquitination (6)					
	Metabolic pathways (37)	Metabolism of nucleotides (6)					
	Oxidative phosphorylation (8)	Kinesins (5)					
	Endocrine and other factor-regulated calcium reabsorption (5)	Disease (24)					
	Pathogenic Escherichia coli infection (9)	Signalling by Rho GTPases (11)					
	Gap junction (6)	RHO GTPase Effectors (9)					
	Protein processing in endoplasmic reticulum (8)	Infectious disease (16)					
	Pyruvate metabolism (4)	Mitotic Anaphase (8)					
	Vascular smooth muscle contraction (7)						

(O) Indicates Observed Gene Count.

3.3. PD-0332991 induced apoptosis

We then investigated the effects of PD-0332991 treatment and miR-21 KO through the Caspase 3/7 activation assay. Caspase-3/7 activity is a crucial step in apoptosis induction, and therefore, a Caspase3/7 activity assay was performed to determine the apoptotic effects of PD-0332991 (2 μ M, for 24 h) treatment and miR-21 deletion in Panc-1 and MiaPaCa-2 PDAC cell lines. We did not detect any apoptotic induction in both Panc-1 and MiaPaCa-2 wt cells treated with PD-0332991 compared to non-treated wt cells. However, PD-0332991 significantly induced apoptosis in Panc-1 miR-21 KO2 and KO4 by 350.4 % and 412.2 %, respectively ($n = 3$; $p \leq 0.01$, for all); and in MiaPaCa-2 miR-21 KO2 and KO4 by 291.8 % and 342.33 %, respectively ($n = 3$; $p \leq 0.01$, for KO2; $p \leq 0.001$, for KO4). Similarly, Panc-1 miR-21 KO2 and KO4 alone, increased Caspase 3/7 activity by 223.5 % and 354.7 %, respectively ($n = 3$; $p \leq 0.05$, for KO2; $p \leq 0.01$, for KO4) (Fig. 6A), whereas MiaPaCa-2 miR-21 KO2 and KO4 alone significantly induced apoptosis by 164.1 % and 250.1 %, respectively ($n = 3$; $p \leq 0.05$, for KO2; $p \leq 0.01$, for KO4) (Fig. 6B).

3.4. PD-0332991 suppressed migration of Panc-1 and MiaPaCa-2 cells and their miR-21 KOs

We tested the cell motility of the PDAC cells treated with/without PD-0332991. For that purpose, the wound-healing assay was performed to confirm the potential effect of PD-0332991 on the migration of Panc-1 and MiaPaCa-2 wt cells and their miR-21 KOs. PD-0332991 treatment alone and combined with miR-21 KO reduced the wound healing capability of cells, while both Panc-1 and MiaPaCa-2 wt cells rapidly closed the wound site (Fig. 7 A, B) within 48 h.

3.5. Mitochondrial bioenergetics of PDAC cells following CDK4/6 inhibition and miR-21 deletion

We further exhibited different metabolic characteristics of PDAC cells, and their miR-21 KOs treated with PD-0332991 by using the Seahorse MitoStress Test. Parameters calculated in the form of bar chart included basal respiration, proton leak, maximal respiration, spare capacity, non-mitochondrial oxygen consumption and ATP-linked respiration (Fig. 8 A, B). In the Panc-1 cells, we observed some alterations in the basal respiration, proton leak, maximal respiration, and spare respiratory capacity of treated with PD-0332991 wt and miR-21 KOs compared to wt cells, however these changes were not significant. There was a decrease by 71.6 % ($n = 3$; $p \leq 0.05$) in the non-mitochondrial oxygen consumption of treated Panc-1 miR-21 KO4 cells (Fig. 8Av) and a reduction by 50.4 % ($n = 3$; $p \leq 0.01$) in the ATP production of Panc-1 miR-21 KO4 in relation to Panc-1 wt cells (Fig. 8Avi). In the MiaPaCa-2 cells, we detected changes in the basal respiration, proton leak and ATP production, however they were non-significant. Compared MiaPaCa-2 miR-21 KO2 and KO4 cells with MiaPaCa-2 wt cells, we detected that miR-21 knockout alone, resulted in the increase of maximal respiratory capacity by 62.53 % and 60.25 %, respectively ($n = 3$; $p \leq 0.05$, for all) (Fig. 8Biii). Furthermore, the non-mitochondrial oxygen consumption of MiaPaCa-2 miR-21 KO2 cells was increased by 102.5 % in comparison to MiaPaCa-2 wt cells ($n = 3$; $p \leq 0.05$) (Fig. 8Biv). Moreover, In the MiaPaCa-2 cell line, there was not an activity in the spare respiratory capacity.

3.6. Proteomic Profiles of PDAC cells and their miR-1 KOs with/without PD-0332991 treatment

Total proteomic content of each group of cells for both Panc-1 and MiaPaCa-2 cell lines were compared using LC-MS/MS analysis. Protein

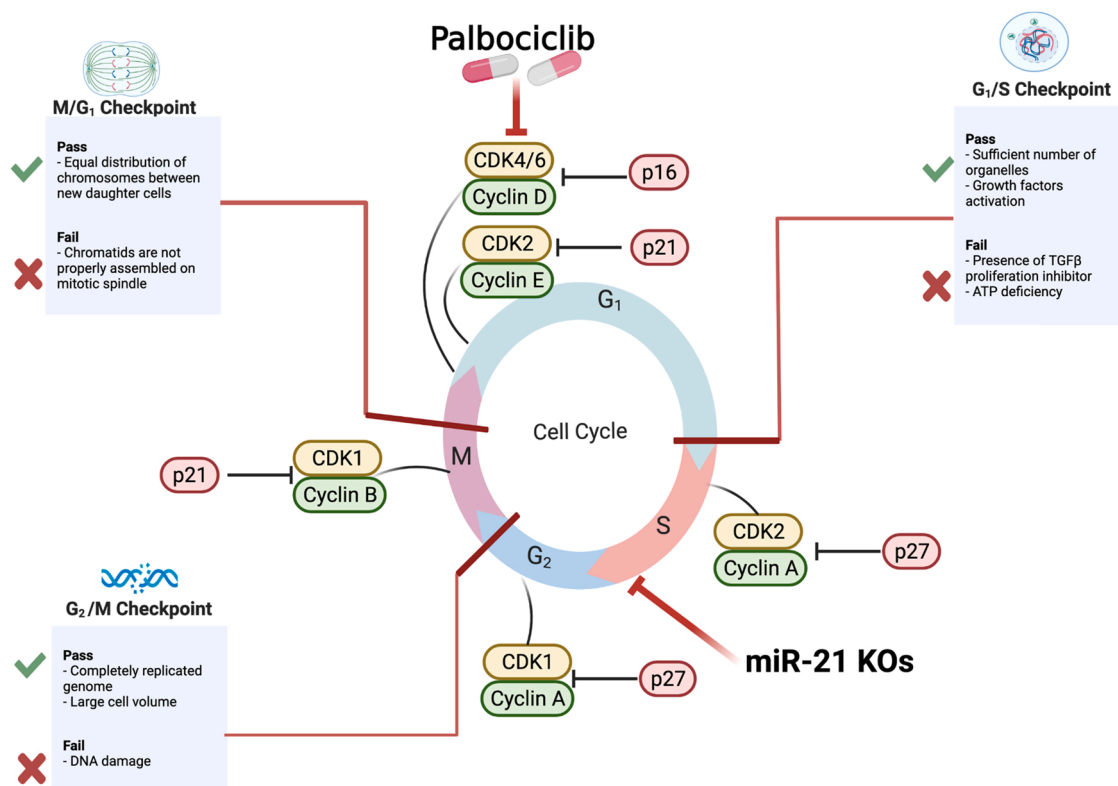


Fig. 11. PD-0332991 and miR-21 KO as coreulatory partners in cell cycle arrest. Cyclins are synthesised in specific phases of the cell cycle and results in the activation of CDKs, and the cyclin-CDK complexes, which regulate progression of the cell throughout the cycle. There are two major classes of CDK inhibitors including the CDK4 (INK4) family (p16^{INK4A}), which blocks the formation of cyclin D-CDK4/6 complexes and the CDK-interacting protein/kinase inhibitory protein family (p21^{Cip1} and p27^{Kip1}), which act on all cyclin-CDK complexes. Initiation of the cell cycle occurs in G₁ phase, which is mainly regulated by the activation of CDK4 and CDK6 kinases that are downstream of mitogenic signals (Baker et al., 2012; Duronio and Xiong, 2013; Morrison, 2012). CDK4 and CDK6 activation are positively moderated through the binding of several D-type cyclins such as cyclin D2, which are highly expressed during G₁/S phase (Pagano et al., 1994). Inhibition of CDK4/6 by using PD-0332991 in combination with miR-21 knockout, can be an effective mechanism of cell cycle arrest in PDAC cells. PD-0332991 blocks cell cycle progression from G₁ to S phase by preventing the CDK4/6-cyclin D1-mediated phosphorylation of RB and is also closely associated with G₂ phase, while PD-0332991 treatment together with miR-21 KO are linked to S and G₂ phases of cell cycle in PDAC. Created with BioRender.com.

hits (shared and unique - from the analysis using the R-script) are shown in Fig. 9 and are further listed and summarised in Supplementary Tables 1–4.

Protein lists for each group were then analysed to STRING (Searching Tool of Retrieval of Interacting Genes/Proteins; <https://string-db.org/>, accessed on October 2022) to illustrate protein-interaction networks and pathway analysis (Fig. 10A, B). KEGG and Reactome specific pathways for each group are presented in Table 3. Additionally, common KEGG pathways between non-treated Panc-1 wt and treated wt include ribosome and metabolic pathways. In MiaPaCa-2 cells, the common KEGG pathway between all subtypes was ribosome; spliceosome was common between MiaPaCa-2 wt and treated wt, whereas KEGG pathway specific to MiaPaCa-2 treated wt and MiaPaCa-2 miR-21 KO2 was mRNA surveillance. Another example of a common KEGG pathway between MiaPaCa-2 treated wt, miR-21 KO2 and treated miR-21 KO2 was RNA transport.

4. Discussion

In this study we analysed the effect of the CDK4/6 inhibitor, PD-0332991, in combination with miR-21 KO. We found that PD-0332991 could be an effective therapeutic strategy for PDAC, affecting not only cell proliferation, viability but also apoptosis.

We showed that PD-0332991 reduced cell viability through regulation of cell survival in both Panc-1 and MiaPaCa-2 cells in line with previous study by Rencuzogullari et al. (2020). We have also found that miR-21 KO alone have decreased cell viability in two different PDAC

cell lines, while PD-0332991 treatment in combination with miR-21 deletion resulted in a higher reduction of cell viability in PDAC. Previously, other studies reported that in vitro inhibition of miR-21 can lead to a significant reduction in cell viability in several cancer types including PDAC (Chan et al., 2005; Meng et al., 2006; Meng et al., 2007; Si et al., 2007). To the best of our knowledge, this is the first time that the synergetic effect of PD-0332991 treatment and miR-21 knocking out in cell viability of PDAC cells, has been studied. Furthermore, our findings provide strong evidence that CDK4/6 inhibition alone and in combination with miR-21 deletion can have subtle effects on the suppression of cellular proliferation in both Panc-1 and MiaPaCa-2 cells. It has been reported that miR-21 plays a key role in cell proliferation of PDAC cells by targeting the MAPK/Extracellular signal-regulated kinase (ERK) and PI3K/AKT signalling pathways (Zhao et al., 2018). Another study indicated that PD-0332991 treatment reduced the colony numbers of Panc-1 and MiaPaCa-2 by 25 % and 15 %, respectively (Sevgin et al., 2021). In our study, for the first time, we showed the combinatory effects of miR-21 deletion with CDK4/6 inhibition that led to reduction of colony formation in PDAC, in vitro. CDK4/6 play a central role in cell-cycle entry and G₁ progression and therefore have been considered as attractive therapeutic targets in numerous tumour types combined with available drugs, which target other cellular pathways (Asghar et al., 2015; Malumbres, 2019; Sherr et al., 2016; Turner et al., 2017). Several studies have noted that the genetic inhibition of CDK4/6 activity can minimise tumour progression in select models (Landis et al., 2006; Malumbres and Barbacid, 2006; Santamaria et al., 2007; Yu et al., 2001). Therefore, the effects on cell cycle arrest following PD-0332991

treatment observed here, may be of some interest. We found that PD-0332991 treatment induced cell cycle arrest at the G1 phase in both Panc-1 and MiaPaCa-2 cells, while synergetic action of PD-0332991 and miR-21 deletion resulted in a more efficient trigger of G1 arrest in vitro. These results are in line with the findings of previous studies, where PD-0332991 promoted cell cycle arrest at the G1 phase and further led to the accumulation of cyclin D1 (Rencuzogullari et al., 2020; Sevgin et al., 2021; Zhang et al., 2017). Previously, it was shown that CDK4/6 inhibition stimulates cytotaxis via cell-cycle arrest in the G1 phase, which has as a further consequence cell growth inhibition (George et al., 2021). Furthermore, in our study we observed that the effective therapeutic potential of PD-0332991 was achieved by reducing the number of PDAC cells in the S phase of cell cycle progression. miR-21 KO alone resulted in suppression of S phase in PDAC cells, however, in combination we found a higher decrease of PDAC cells number in S phase. It has been demonstrated that upregulation of miR-21 prompted the transition from G0/G1 phase to S phase under epidermal growth factor (EGF) stimulation in PDAC, therefore, miR-21 may play a regulatory role in the inducement of G1/S transition in PDAC (Zhao et al., 2018). Moreover, based on our current study, the synergetic effect of PD-0332991 treatment and miR-21 deletion arrests PDAC cells in the G2-phase, which has been demonstrated in a similar trend with previous studies (Rencuzogullari et al., 2020; Sevgin et al., 2021). Cyclin-CDK complexes moderate cell cycle through the phosphorylation of RB and has as a result the suppression of E2F transcription factor family that allows cells to divide (O'Leary et al., 2016). The CDK4/6 inhibitors act at the G₁-to-S cell cycle checkpoint and this checkpoint is moderated through D-type cyclins CDK4 and CDK6 (O'Leary et al., 2016), which prevent the phosphorylation of RB protein (George et al., 2021). Further non-cell cycle related effects of CDK4/6 include direct activation of vascular endothelial growth factor (VEGF) transcription, promotion of angiogenesis and nuclear factor (NF)- κ B activation via the p65 transcription factor (Abedin et al., 2010; Handschick et al., 2014; Kollmann et al., 2013). The need of developing effective therapeutic strategies based on CDK4/6 inhibitors in combination with other agents, which are clinically active, is vital (Fig. 11).

Importantly, a previous in vitro study reported that Panc-1 and MiaPaCa-2 cells treated with PD-0332991 stained positively with SA- β Gal, which indicates the inducer role of PD-0332991 in terms of senescence (Sevgin et al., 2021). This finding is consistent with our study, which revealed that PD-0332991 alone and in combination with miR-21 deletion triggered cellular senescence in two different PDAC cell lines. Several studies have shown that several miRs including miR-21 are differentially expressed in senescent cells and play a regulatory role in cellular senescence (Creemers et al., 2012; Jung and Suh, 2014; Williams et al., 2017). Particularly, miR-21 level is upregulated during the ageing process and linked to various malignancies including PDAC (Lee et al., 2007; Nakata et al., 2011; Olivieri et al., 2017). Popov and Mandys (2022) reported that miR-21 is a senescence-associated miRs (SA-miRs), which control cell transition during cell cycle (G1/S or G2/M checkpoints) through targeting CDKs and CDK inhibitors (Bueno and Malumbres, 2011). Moreover, a previous study has indicated that cyclin D-CDK4/6 complexes lead to the phosphorylation and FOXM1, which protects cancer cells from senescence (Anders et al., 2011). Furthermore, it has been described previously that inhibition of CDK4/6 in preclinical models leads to the activation of RB, which can further induce senescent-like arrest (Dean et al., 2012a; Dean et al., 2012b; Finn et al., 2009; Fry et al., 2004; Konecny et al., 2011; McClendon et al., 2012; Toogood et al., 2005).

According to a recent study, almost all CDK4/6 inhibitors, including PD-0332991 can induce apoptosis in numerous malignancies (Franco et al., 2014). Moreover, cyclin D-CDK4/6 complexes also contribute not only in apoptosis but also in glucose metabolism and cell differentiation (Hydbring et al., 2016; Lee et al., 2014). We found that PD-0332991 treatment induced higher apoptotic rate in both Panc-1 and MiaPaCa-2 miR-21 KO cells but not in their treated wt cells, whereas miR-21

KOs alone triggered apoptosis in PDAC cells. Similarly, a previous study showed that miR-21 overexpression results in the prevention of apoptosis (Park et al., 2009), and Buscaglia, Li (2011) reviewed that miR-21 is closely associated with several stages of oncogenic life including stimulation of cell proliferation, invasion and metastasis, genome instability inflammation, immune destruction, abnormal metabolism, angiogenesis, and suppression of apoptosis. Further studies have also revealed that CDK4/6 inhibitors contribute to tumour cell apoptosis (Helsten et al., 2016; Minton, 2017), while a similar study determined that CDK4/6 inhibitors can stimulate not only caspase-dependent apoptosis through the regulation of Bax and Bak proteins in MiaPaCa-2 cells but also caspase-independent apoptosis in Panc-1 cells through raised cleavage of Poly (ADP-ribose) polymerase (PARP) (Sevgin et al., 2021).

Overexpression of miR-21 promotes cell invasion in PDAC, while inhibition of miR-21 reduces cell proliferation, invasion, and chemoresistance for gemcitabine (Moriyama et al., 2009). In our study, we found that the combination of PD-0332991 and miR-21 KO cells decreased the cell motility significantly when used in combination. Further studies investigated that miR-21 expression is related to invasion-related genes such as VEGF (Wey et al., 2005). Previously, it has been shown that PD-0332991 suppressed migration and invasion in esophageal squamous cell carcinoma (ESCC) cells (Chen and Pan, 2017).

Mitochondria are key regulators of cellular energy metabolism, with mitochondrial respiration generating most of the intracellular ATP. Therefore, we assessed the key parameters of mitochondrial respiration in PDAC cells following PD-0332991 treatment and miR-21 knocking out. Specifically, basal respiration represents the energetic demand of cells under basal conditions, the oxygen consumption of basal respiration used to meet ATP synthesis and leads to mitochondrial proton leak. ATP-linked respiration is associated with the reduction in OCR after the injection of the oligomycin, which is the portion of basal respiration. Proton leak can be described as the remaining basal respiration, which has not coupled to ATP synthesis after oligomycin injection and can be a sign of mitochondrial damage. Additionally, maximal respiration represents the maximum capacity that the electron respiratory chain can achieve and is measured by the injection of the uncoupler FCCP. We revealed that MiaPaCa-2 miR-21 KO2 and KO4 increased maximal respiration compared to MiaPaCa-2 wt cells, whereas a previous study showed that anti-miR-21-5p-transfected H9C2 cells presented a high increase in maximal respiration (Nasci et al., 2019). Spare respiration is the difference between maximal and basal respiration, which indicates the ability of the PDAC cells to respond to alterations in energetic demand and demonstrates the fitness of the PDAC cells. Besides, non-mitochondrial respiration is the oxygen consumption caused by cellular enzymes and not mitochondria after the injection of rotenone and antimycin A (Gu et al., 2021). In our study, we found slight changes in the basal respiration, proton leak and spare respiratory capacity rates (albeit all non-significant). This might be explained by the high variability between the different biological repeats and wells in each experiment and by interventions that were introduced to the cells such as miR-21 deletion and compound treatments (PD-0332991), which can have as a further result change in the cell numbers during the culture. One further explanation could be the unequal distribution of cells within the well, and particularly, in the centre of the well, where the Seahorse microchamber measures oxygen concentration (Little et al., 2020).

In this current study, we assessed the proteomic profiles of two different PDAC cell lines (Panc-1 and MiaPaCa-2) following PD-0332991 treatment and miR-21 knock-out, compared with Panc-1 and MiaPaCa-2 wt cells. We identified large-scale proteomic signatures between wt and treated cells. Moreover, to further understand changes in the pathological and physiological pathways associated with Panc-1 and MiaPaCa-2 wt cells versus treated with PD-0332991 and miR-21 KO2s, protein-protein interaction network analysis was carried out. Several KEGG pathways were identified as specific to the total proteomic profile of Panc-1 wt, including vibrio cholerae infection and RNA transport,

while specific KEGG pathways for Panc-1 treated wt comprised citrate cycle, pyruvate metabolism, peroxisome, long-term depression, endocrine and factor regulated calcium reabsorption, carbon metabolism, gap junction, oxidative phosphorylation, vascular smooth muscle contraction, pathogenic *E.coli* infection, protein processing in endoplasmic reticulum and Huntington disease. A recent study has revealed that PD-0332991 can result in the dysregulation of metabolites in several metabolic pathways in central carbon metabolism in breast cancer cells (Warth et al., 2019), whereas PD-0332991 can also affect the regulation of the isoform M2 of pyruvate kinase (PKM2) (Amelio et al., 2014). In addition, Reactome pathways relating specific to Panc-1 miR-21 KO2 included kinesins, protein ubiquitination, metabolism of nucleotides, mitotic anaphase, cell cycle (mitotic), M phase, cell cycle, RHO GTPase effectors, signalling by Rho GTPases, infectious disease, post-translational protein modification, metabolism of proteins and disease. Particularly, miR-21 can moderate cellular proliferation, migration, invasion, metastasis, and survival through the inhibition of tumour suppressor RhoB in colorectal and breast cancer (Connolly et al., 2010; Liu et al., 2011). PD-0332991 can promote G0/G1 cell cycle arrest through the inducement of senescence in fibroblasts, breast cancer, and melanoma cells (Jost et al., 2021). Furthermore, Reactome pathways particular for the Panc-1 treated miR-21 KO2 were Golgi associated-vesicle biogenesis, programmed cell death, membrane trafficking and immune system. A recent study has indicated that miR-21 controls the apoptosis of cervical cancer cells by tumour necrosis factor- α (Xu et al., 2017). Specific KEGG pathway for MiaPaCa-2 treated wt cells was RNA degradation and for MiaPaCa-2 miR-21 KO2 were *Vibrio cholerae* infection and synaptic vesicle cycle. A previous study showed that numerous miRs can regulate synaptic mRNA expression (Paschou et al., 2012). Additionally, metabolic pathways were specific for MiaPaCa-2 miR-21 KO2 treated with PD-0332991, whereas no KEGG pathways were specific to the MiaPaCa-2 wt cells proteome.

5. Conclusions

In conclusion, we found that PD-0332991 could be used as a promising candidate for combined drug therapy in PDAC. Moreover, our present study showed a novel function of miR-21 KO2 in the regulation of cell cycle progression, cell proliferation, apoptosis, and senescence, which may provide a therapeutic potential for PDAC in combination with PD-0332991 treatment. Therefore, our study provides preliminary mechanistic insights of PD-0332991, which can be used as a clinical evaluation for PDAC therapy, as the administration of PD-0332991 as a single agent is not sufficient enough to decrease poor progression of PDAC cells. Further studies are needed to understand how specific tissue and serum biomarkers could predict the effectiveness of this CDK4/6 inhibitor to provide optimal treatment combinations.

Funding

This work partially was supported by the University of Westminster SLS Ph.D. studentships to M.M.

CRediT authorship contribution statement

Maria Mortoglou: writing— original draft preparation, investigation, methodology. **Francesc Miralles:** Editing, investigation and reviewing **Rhys Richard Mould:** Editing and reviewing **Dipankar Sengupta:** Editing and reviewing. **Pinar Uysal-Onganer:** writing— original draft preparation, review and editing, funding acquisition, formal analysis, validation, investigation, methodology, supervision. All authors have read and agreed to the published version of the manuscript.

Declaration of Competing Interest

The authors declare that they have no known competing financial interests or personal relationships that could have appeared to influence the work reported in this paper.

Data Availability

Data will be made available on request.

Acknowledgments

The authors would like to thank Junming Yue, University of Tennessee Health Science Center, USA, for donating the lentiviral CRISPR/Cas9-mediated miR-21 gene editing vectors and control vector.

Appendix A. Supporting information

Supplementary data associated with this article can be found in the online version at doi:10.1016/j.ejcb.2023.151318.

References

- Abedin, Z.R., Ma, Z., Reddy, E.P., 2010. Increased angiogenesis in Cdk4- (R24C/R24C): Apc(+/-Min) intestinal tumors. *Cell Cycle* 9 (12), 2456–2463. <https://doi.org/10.4161/cc.9.12.12055>.
- Amelio, I., Cutruzzola, F., Antonov, A., Agostini, M., Melino, G., 2014. Serine and glycine metabolism in cancer, 2014 *Trends Biochem. Sci.* 39, 191–198. <https://doi.org/10.1016/j.tibs.2014.02.004>.
- Anders, L., Ke, N., Hydrbring, P., Choi, Y., Widlund, H., Chick, J.M., Zhai, H., Vidal, M., Gygi, S.P., Braun, P., Sicinski, P., 2011. A systematic screen for CDK4/6 substrates links FOXM1 phosphorylation to senescence suppression in cancer cells, 2011 *Cancer Cell* 20, 620–634. <https://doi.org/10.1016/j.ccr.2011.10.001>.
- Arisan, E.D., Rencuzogullari, O., Cieza-Borrella, C., Miralles Arenas, F., Dwek, M., Lange, S., Uysal-Onganer, P., 2021. MiR-21 is required for the epithelial–mesenchymal transition in MDA-MB-231 breast cancer cells. *Int. J. Mol. Sci.* 22 (2021), 1557. <https://doi.org/10.3390/ijms22041557>.
- Asangani, I.A., Rasheed, S.A., Nikolova, D.A., Leupold, J.H., Colburn, N.H., Post, S., Allgayer, H., 2008. MicroRNA-21 (miR-21) post-transcriptionally downregulates tumor suppressor Pcd4 and stimulates invasion, intravasation and metastasis in colorectal cancer. *Oncogene* 27 (2008), 2128–2136. <https://doi.org/10.1038/sj.onc.1210856>.
- Asghar, U., Witkiewicz, A.K., Turner, N.C., Knudsen, E.S., 2015. The history and future of targeting cyclin-dependent kinases in cancer therapy. *Nat. Rev. Drug Discov.* 14 (2015), 130–146. <https://doi.org/10.1038/nrd4504>.
- Bailey, J.M., Hendley, A.M., Lafaro, K.J., Pruski, M.A., Jones, N.C., Alsin, J., Younes, M., Maitra, A., McAllister, F., Iacobuzio-Donahue, C.A., Leach, S.D., 2016a. P53 mutations cooperate with oncogenic kras to promote adenocarcinoma from pancreatic ductal cells. *Oncogene* 35 (2016b), 4282–4288. <https://doi.org/10.1038/nc.2015.441>.
- Bailey, P., Chang, D.K., Nones, K., Johns, A.L., Patch, A.M., Gingras, M.C., Miller, D.K., Christ, A.N., Bruxner, T.J., Quinn, M.C., et al., 2016b. Genomic analyses identify molecular subtypes of pancreatic cancer. *Nature* 531 (2016a), 47–52. <https://doi.org/10.1038/nature16965>.
- Baker, S.J., Reddy, E.P., 2012. A key player in the cell cycle. *Dev. Cancer Genes Cancer* 3 (11–12), 658–669. <https://doi.org/10.1177/1947601913478972>.
- Biankin, A.V., Waddell, N., Kassahn, K.S., Gingras, M.C., Muthuswamy, L.B., Johns, A.L., Miller, D.K., Wilson, P.J., Patch, A.M., Wu, J., et al., 2012. Pancreatic cancer genomes reveal aberrations in axon guidance pathway genes. *Nature* 491 (2012), 399–405. <https://doi.org/10.1038/nature11547>.
- Bonelli, M., La Monica, S., Fumarola, C., Alfieri, R., 2019. Multiple effects of CDK4/6 inhibition in cancer: from cell cycle arrest to immunomodulation. *Biochem. Pharmacol.* 170, 113676 <https://doi.org/10.1016/j.bcp.2019.113676>.
- Bryant, K.L., Mancias, J.D., Kimmelman, A.C., Der, C.J., 2014. KRAS: Feeding pancreatic cancer proliferation. *Trends Biochem. Sci.* 39 (2014), 91–100. <https://doi.org/10.1016/j.tibs.2013.12.004>.
- Bueno, M.J., Malumbres, M., 2011. MicroRNAs and the cell cycle. *Biochim Biophys. Acta Mol. Basis Dis.* 1812 (2011), 592–601. <https://doi.org/10.1016/j.bbdis.2011.02.002>.
- Buscaglia, L.E., Li, Y., 2011. Apoptosis and the target genes of microRNA-21, 2011 *Chin. J. Cancer* 30 (6), 371–380. <https://doi.org/10.5732/cjc.011.10132>.
- Cancer Genome Atlas, 2017. Cancer genome atlas research network integrated genomic characterization of pancreatic ductal adenocarcinoma, 2017 *Cancer Cell* 32 (2), 185–203. <https://doi.org/10.1016/j.ccell.2017.07.007>.
- Chan, J.A., Krichevsky, A.M., Kosik, K.S., 2005. MicroRNA-21 is an antiapoptotic factor in human glioblastoma cells. *Cancer Res* 65 (2005), 6029–6033. <https://doi.org/10.1158/0008-5472.CAN-05-0137>.

- sequencing of pancreatic cancer defines genetic diversity and therapeutic targets. *Nat. Commun.* 6 (2015a), 6744. <https://doi.org/10.1038/ncomms7744>.
- Witkiewicz, A.K., Borja, N.A., Franco, J., Brody, J.R., Yeo, C.J., Mansour, J., Choti, M.A., McCue, P., Knudsen, E.S., 2015b. Selective impact of CDK4/6 suppression on patient-derived models of pancreatic cancer. *Oncotarget* 6 (2015b), 15788–15801.
- Xu, L., Xu, Q., Li, X., Zhang, X., 2017. MicroRNA-21 regulates the proliferation and apoptosis of cervical cancer cells via tumor necrosis factor- α . 2017 *Mol. Med. Rep.* 16 (4), 4659–4663. <https://doi.org/10.3892/mmr.2017.7143>.
- Young, R.J., Waldeck, K., Martin, C., Foo, J.H., Cameron, D.P., Kirby, L., Do, H., Mitchell, C., Cullinane, C., Liu, W., et al., 2014. Loss of CDKN2A expression is a frequent event in primary invasive melanoma and correlates with sensitivity to the CDK4/6 inhibitor PD0332991 in melanoma cell lines, 2014 *Pigment. Cell Melanoma Res.* 27 (4), 590–600. <https://doi.org/10.1111/pcmr.12228>.
- Yu, Q., Geng, Y., Sicinski, P., 2001. Specific protection against breast cancers by cyclin D1 ablation, 2001 *Nature* 411 (6841), 1017–1021. <https://doi.org/10.1038/35082500>.
- Yue, J., Sheng, Y., Ren, A., Penmatsa, S., 2010. A miR-21 hairpin structure-based gene knockdown vector. *Biochem. Biophys. Res. Commun.* 394 (2010), 667–672. <https://doi.org/10.1016/j.bbrc.2010.03.047>.
- Yuedi, D., Houbao, L., Pinxiang, L., Hui, W., Min, T., Dexiang, Z., 2020. KLF2 induces the senescence of pancreatic cancer cells by cooperating with FOXO4 to upregulate p21, 2020 *Exp. Cell Res.* 388 (1), 111784. <https://doi.org/10.1016/j.yexcr.2019.111784>.
- Zhang, J., Zhou, L., Zhao, S., Dicker, D.T., El-Deiry, W.S., 2017. The CDK4/6 inhibitor palbociclib synergizes with irinotecan to promote colorectal cancer cell death under hypoxia, 2017 *Cell Cycle* 16 (12), 1193–1200. <https://doi.org/10.1080/15384101.2017.1320005>.
- Zhao, Q., Chen, S., Zhu, Z., Yu, L., Ren, Y., Jiang, M., Weng, J., Li, B., 2018. miR-21 promotes EGF-induced pancreatic cancer cell proliferation by targeting Spry2. *Cell Death Dis.* 9 (2018), 1157. <https://doi.org/10.1038/s41419-018-1182-9>.
- Zhou, X., Zhou, X., Wang, X., Huang, Z., Wang, J., Zhu, W., Shu, Y., Liu, P., 2014. Prognostic value of miR-21 in various cancers: an updating meta-analysis, 2014 *PLoS One* 9 (7), e102413. <https://doi.org/10.1371/journal.pone.0102413>.